

Fate of Electroweak Vacuum during Preheating

Yohei Ema[◇], Kyohei Mukaida[◇], Kazunori Nakayama^{◇,◇}

- ◇ *Department of Physics, Faculty of Science,
The University of Tokyo, Bunkyo-ku, Tokyo 133-0033, Japan*
- ◇ *Kavli IPMU (WPI), UTIAS,
The University of Tokyo, Kashiwa, Chiba 277-8583, Japan*

Abstract

Our electroweak vacuum may be metastable in light of the current experimental data of the Higgs/top quark mass. If this is really the case, high-scale inflation models require a stabilization mechanism of our vacuum during inflation. A possible candidate is the Higgs-inflaton/-curvature coupling because it induces an additional mass term to the Higgs during the slow roll regime. However, after inflation, the additional mass term oscillates, and it can destabilize our electroweak vacuum via production of large Higgs fluctuations during the inflaton oscillation era. In this paper, we study whether or not the Higgs-inflaton/-curvature coupling can save our vacuum by properly taking account of Higgs production during the preheating stage. We put upper bounds on the Higgs-inflaton and -curvature couplings, and discuss possible dynamics that might relax them.

Contents

1	Introduction and Summary	1
1.1	Introduction	1
1.2	Summary	2
2	Higgs-Inflaton Coupling	3
2.1	Preheating via quartic stabilization: $c^2\phi^2h^2$	7
2.2	Preheating via curvature stabilization: ξRh^2	12
3	Higgs-Radiation Coupling	17
3.1	Instant preheating	18
3.2	Annihilation	20
4	After Preheating	23
4.1	Cosmic expansion	24
4.2	Turbulence and thermalization	24
4.3	Complete reheating	25
5	Conclusions and Discussion	27
A	Mode Expansion	30
B	Renormalization in Classical Lattice Simulation	31
C	Thermalization after Inflation	32

1 Introduction and Summary

1.1 Introduction

The current measurements of the Higgs and top quark masses suggest that the Higgs quartic coupling flips its sign well below the Planck scale if there is no new physics other than the Standard Model (SM) [1–14]. It indicates that there may be a true vacuum at a large Higgs field value region, and our electroweak vacuum may not be absolutely stable. Since its lifetime is much longer than the age of the Universe, the electroweak vacuum is metastable for the best fit values of SM parameters.^{♥1} In this paper, we take this situation seriously, assuming the metastable electroweak vacuum.

In the cosmological context, an interesting consequence of the Higgs metastability is that high-scale inflation has a tension with it [7, 18–24]. This is because Higgs acquires fluctuations of the order of the Hubble parameter H_{inf} during inflation. As a result, the Higgs field falls into a lower potential energy region, and the electroweak vacuum decays if the inflation scale is high enough. Therefore, some stabilization mechanism of Higgs is necessary for high-scale inflation scenarios to be consistent with the metastable electroweak vacuum. A leading candidate of such a stabilization mechanism is the following Higgs-inflaton/-curvature interaction:

$$\mathcal{L}_{\text{int}}(\phi, h) = \begin{cases} -\frac{1}{2}c^2\phi^2h^2, \\ -\frac{1}{2}\xi R h^2, \end{cases} \quad (1.1)$$

where ϕ is the inflaton field, h is a radial component of the Higgs field and R is the Ricci scalar. Higgs acquires an effective mass term from this interaction during inflation, and hence the Higgs fluctuations are suppressed if the conditions $c^2\phi_{\text{inf}}^2, \xi R_{\text{inf}} \gtrsim H_{\text{inf}}^2$ are satisfied. Thus, the interaction (1.1) can stabilize the electroweak vacuum during inflation.

However, in such a case, the interaction (1.1) itself makes the dynamics during the preheating stage^{♥2} highly nontrivial. The Higgs-inflaton quartic coupling causes the broad resonance of Higgs [25, 26] due to the breakdown of its adiabaticity and its Bose enhancement. As a result, the fluctuations of Higgs grow exponentially.^{♥3} The Higgs-curvature coupling causes a tachyonic enhancement of Higgs [30–32] because the curvature-induced effective mass squared becomes negative for some period during one oscillation of the inflaton. Thus, the exponential growth of Higgs fluctuations may force our electroweak vacuum to decay into the true one during the preheating stage. The interaction (1.1) may eventually fail to save the electroweak vacuum.

In this paper, we focus on the dynamics of Higgs during the preheating caused by the interaction (1.1). The main purpose of this paper is to investigate in what parameter space the interaction (1.1) does not trigger the electroweak vacuum decay during the preheating stage. We use both analytical and numerical methods to study the effects of the broad/tachyonic resonance on the Higgs metastability. We also consider the interactions between Higgs and radiation composed of other SM particles during preheating. In addition, we discuss possible dynamics of Higgs after the resonance shuts off, that is to say, after the preheating. In the

^{♥1} Higher dimensional operators may shorten the lifetime of the electroweak vacuum [15–17].

^{♥2} A note on terminology. In this paper, the word “preheating” represents the epoch in which some resonant particle production processes occur due to the inflaton oscillation after inflation.

^{♥3} See also Refs. [27–29].

next sub-section, we summarize main results of this paper for the convenience of readers. We also give the organization of this paper there.

1.2 Summary

Here main results of this paper are summarized. We study evolution of Higgs during the preheating stage driven by the interaction (1.1), and obtain the parameter region in which Higgs remains in the electroweak vacuum during the preheating. To be more specific, the electroweak vacuum survives the preheating stage if the couplings satisfy the following inequalities.

Upper bounds on Higgs-inflaton and -curvature couplings:

$$c \lesssim 10^{-4} \left[\frac{0.1}{\mu_{\text{qtc}}} \right] \left[\frac{m_\phi}{10^{13} \text{ GeV}} \right], \quad (1.2)$$

for the quartic coupling case, and

$$\xi \lesssim 10 \left[\frac{2}{n_{\text{eff}} \mu_{\text{crv}}} \right]^2 \left[\frac{\sqrt{2} M_{\text{pl}}}{\Phi_{\text{ini}}} \right]^2, \quad (1.3)$$

for the curvature coupling case.

Here m_ϕ is the inflaton mass, Φ_{ini} is the initial inflaton amplitude at the beginning of its oscillation, M_{pl} is the reduced Planck mass, n_{eff} is an effective number of oscillation [See the text below Eq. (2.42)], $\mu_{\text{qtc}} \simeq 0.1$ and $\mu_{\text{crv}} \simeq 2$. See also Eqs. (2.29) and (2.44). For simplicity, we assume that inflaton oscillates with a quadratic potential to derive these bounds. We obtain the upper bounds from the requirement that the Hubble expansion should kill the broad/tachyonic resonance before Higgs escapes from the electroweak vacuum. See Sec. 2 for details. In order to confirm these upper bounds, we perform classical lattice simulations. Effects of other SM particles are discussed in Sec. 3 and also in the first part of Sec. 4.3. The couplings c and ξ should satisfy $c \gtrsim \mathcal{O}(H_{\text{inf}}/\Phi_{\text{ini}})$ and $\xi \gtrsim \mathcal{O}(0.1)$ [7, 24] to suppress the Higgs fluctuations during inflation. Thus, our result indicates that the allowed values of the couplings lie in a rather narrow band, for the stability of Higgs during both the inflation and the preheating stages.

After the preheating, the dynamics of Higgs becomes quite complicated once we include the interactions among Higgs, top quark and SM gauge bosons. If we ignore this interaction, the bounds on the couplings become severer than Eqs. (1.2) and (1.3). This is because the cosmic expansion reduces the Higgs effective mass induced from Eq. (1.1) much faster than the tachyonic mass induced from its self interaction [See Eqs. (4.4) and (4.5)]. Thus, it is essential to include the interaction among Higgs and SM particles so as to discuss the fate of electroweak vacuum after the preheating. One possible fate is that, after the electroweak vacuum survives the preheating stage, Higgs thermalizes with the other SM particles. Once it is thermalized, the life time of our vacuum can be estimated by means of the bounce method under a periodic Euclidean time [33, 34]. For thermalized radiation, the electroweak vacuum does not decay after the preheating even with a temperature $T \sim M_{\text{pl}}$ for the central value

of the top quark mass [35]. See discussion in Sec. 4.2. Also, the direct decay of inflaton into other SM particles, which is responsible for the complete reheating, would play essential roles. Typically, a larger reheating temperature tends to stabilize the electroweak vacuum, while a smaller one does not play the role. See discussion in Sec. 4.3. Also, resonant production of other SM particles during the early stage of complete reheating, if any, might affect the bounds given in Eqs. (1.2) and (1.3). However, above mechanisms strongly depends on thermalization processes. A detailed study on the dynamics of Higgs after the preheating, including Higgs-radiation and inflaton-radiation couplings, is left for a future work.

The organization of this paper is as follows. In Sec. 2, we first shut off the Higgs-radiation couplings and focus on the Higgs-inflaton/-curvature coupling during the preheating regime. We study effects of the broad/tachyonic resonance on the electroweak vacuum stability both analytically and numerically. Then, in Sec. 3, we turn on the Higgs-radiation coupling, and investigate how it could modify results of the previous sections. We will see that it is expected to be less significant during the preheating. In Sec. 4, we discuss a possible fate of the electroweak vacuum after the preheating. At the end of Sec. 4, we discuss how the decay of inflaton into other SM particles could change the results. The last section is devoted to the conclusion and the discussion.

2 Higgs-Inflaton Coupling

The main goal of our study here is to estimate the Higgs-inflaton/-curvature coupling strength below which the electroweak vacuum survives the preheating stage. In particular, we will make it clear in what condition the electroweak vacuum does not decay albeit the resonance occurs at the beginning of the inflaton oscillation. In order to achieve this goal, we use both analytical and numerical methods. The essential point here is that the coupling cannot be arbitrarily small in order to suppress the Higgs fluctuation during inflation.

First, let us explain our setup. In this section, we shut off the Higgs-radiation couplings, *i.e.* gauge and top Yukawa couplings, so as to clarify the role of Higgs-inflaton and -curvature couplings in the preheating stage. We study the following model throughout this section:^{∇4}

$$\mathcal{L} = \mathcal{L}_{\text{inf}}(\phi) + \mathcal{L}_{\text{Higgs}}(h) + \mathcal{L}_{\text{int}}(\phi, h), \quad (2.1)$$

where \mathcal{L}_{inf} , $\mathcal{L}_{\text{Higgs}}$ and \mathcal{L}_{int} are the Lagrangian densities of the inflaton sector, the Higgs sector and the interaction between inflaton/curvature and Higgs, respectively. We take the inflaton sector as

$$\mathcal{L}_{\text{inf}}(\phi) = \frac{1}{2} \partial_\mu \phi \partial^\mu \phi - \frac{1}{2} m_\phi^2 \phi^2, \quad (2.2)$$

where we have assumed that the inflaton potential around its origin is quadratic. Note that, although the simple chaotic inflation model with a quadratic potential is excluded by observations [36], it is possible to modify the large field behavior to make it consistent with observations (see *e.g.* Refs. [37–42]). We implicitly assume this in the following. The Higgs sector is given by

$$\mathcal{L}_{\text{Higgs}}(h) = \frac{1}{2} \partial_\mu h \partial^\mu h - \frac{1}{4} \lambda(\mu) h^4, \quad (2.3)$$

^{∇4} For simplicity, we treat Higgs as a one component field here. However, our constraints derived from now are not sensitive to it because they depend only logarithmically on the number of components.

where μ is the renormalization scale. Here we have dropped the negative Higgs mass squared since it is irrelevant for our following discussion. We roughly approximate the Higgs self coupling $\lambda(\mu)$ as

$$\lambda(\mu) \simeq \tilde{\lambda} \text{sign}(h_{\max} - \mu); \quad \text{with } \tilde{\lambda} \simeq 0.01. \quad (2.4)$$

See Refs. [13, 14] for the running of the Higgs four point coupling. The scale h_{\max} , where the Higgs quartic coupling becomes negative, significantly depends on the top quark mass. For its current central value, it is given by $h_{\max} \simeq 10^{10}$ GeV [14]. For the interaction term which induces a sizable effective mass of Higgs during inflation, we consider two different interactions as representative models:

$$\mathcal{L}_{\text{int}}(\phi, h) = \begin{cases} -\frac{1}{2} c^2 \phi^2 h^2 & \dots \text{quartic,} \\ -\frac{1}{2} \xi R h^2 & \dots \text{curvature.} \end{cases} \quad (2.5)$$

Here we comment on the renormalization scale μ . There are two relevant physical scales in the following discussion, *i.e.* a typical momentum scale of preheating p_* defined later and the dispersion of Higgs $\sqrt{\langle h^2 \rangle}^{\heartsuit 5}$ since we deal with an inhomogeneous Higgs field owing to Higgs particle production. Thus, it is nontrivial which one we should choose as the renormalization scale for the vacuum decay triggered by the preheating dynamics. Fortunately, however, our results are *insensitive* to this choice as long as $m_\phi \gg h_{\max}$. This is because, even if we set $\mu = \sqrt{\langle h^2 \rangle}$ and hence start with positive λ , a sizable Higgs dispersion, $\langle h^2 \rangle \sim p_*^2 \gtrsim m_\phi^2$, is produced right after the first oscillation of inflaton in the case of our interest. Therefore, the self coupling λ becomes negative just after the first oscillation. As a result, the dynamics is the same as that with $\mu = p_*$ ($\gtrsim m_\phi$), or the case where λ is negative from the beginning. For a classical lattice simulation, we take the renormalization scale as $\mu = \text{Max}[h, p_*]^{\heartsuit 6}$ but readers should keep in mind the insensitivity of our result to this choice.^{\heartsuit 7}

In the following, we study the preheating epoch driven by the Higgs-inflaton/-curvature interaction (2.5) separately. We first discuss qualitative behavior of the system, and in particular clarify the condition where the Higgs field rolls down to the lower potential energy regime than the electroweak vacuum. Then, we show results of numerical simulations and confirm our qualitative understanding. In the subsequent sections, we will turn on the Higgs-radiation coupling and discuss how it affects the fate of the electroweak vacuum. For that purpose, it is helpful to understand the dynamics qualitatively at first, so that we can apply our understandings to more complicated systems.

^{\heartsuit 5} One might think of the Hubble parameter H as another choice, for it would be the scale for the long wave length mode. Even if it is the correct choice, our results do not change as long as $H > h_{\max}$ is satisfied for the first $\mathcal{O}(10)$ times of inflaton-oscillation.

^{\heartsuit 6} As can be inferred from Eqs. (2.26) and (2.43), not only the long wave length mode but all the modes of Higgs below the typical scale p_* are relevant when the vacuum decay is triggered. (Precisely speaking, in the case of the curvature coupling, the scale is much larger; $q^{1/4} p_*$.) This is because the conditions [Eqs. (2.26) and (2.43)] indicate that all the modes below p_* overcome the pressure of spacial gradients of p_*^{-1} owing to the tachyonic effective mass term. This is the reason why we take this criterion.

^{\heartsuit 7} The rescatterings of produced Higgs particles via the “positive” four point coupling may kill the resonance, if $p_*^2 < \lambda \langle h^2 \rangle$ under $\sqrt{\langle h^2 \rangle} < h_{\max}$. This is the case for $\lambda > p_*^2 / h_{\max}^2 > m_\phi^2 / h_{\max}^2$. In the second inequality, we have used $p_* > m_\phi$ in Eq. (2.20) [or (2.41)]. It means that h_{\max} has to be much larger than m_ϕ at least for the perturbative λ . Since we are interested in the opposite case $h_{\max} \ll m_\phi$, we can safely just take λ to be negative in the simulation.

Preliminaries

Before moving to each case, we summarize common features of this system. At first, we can safely neglect effects of Higgs fluctuations on the inflaton dynamics since there are no particles right after the inflation. Then, the inflaton obeys the following approximated solution:

$$\phi(t) \simeq \Phi(t) \cos(m_\phi t); \quad \Phi(t) = \frac{\Phi_{\text{ini}}}{a^{\frac{3}{2}}(t)}, \quad (2.6)$$

where $a(t) \propto t^{2/3}$ is the scale factor, and $\Phi(t)$ is an inflaton amplitude with Φ_{ini} being its initial value at the onset of the inflaton oscillation. Correspondingly, the dispersion relation of Higgs also oscillates with time, and the Higgs field acquires fluctuations as we shall see below.

Let us start with a mode expansion of the Higgs field:

$$h(x) = \int \frac{d^3k}{[2\pi a(t)]^{3/2}} [\hat{a}_{\mathbf{k}} h_{\mathbf{k}}(t) e^{i\mathbf{k}\cdot\mathbf{x}} + \text{H.c.}], \quad (2.7)$$

where \mathbf{k} is a comoving momentum and $a(t)$ is the scale factor. Neglecting interaction terms, we find the equation of motion for the wave function $h_{\mathbf{k}}$:

$$0 = \ddot{h}_{\mathbf{k}}(t) + [\omega_{\mathbf{k};h}^2(t) + \Delta(t)] h_{\mathbf{k}}(t), \quad (2.8)$$

where $\Delta \equiv -9H^2/4 - 3\dot{H}/2$, $H \equiv \dot{a}/a$ is the Hubble parameter, and $\omega_{\mathbf{k};h}(t)$ is the time dependent dispersion relation of Higgs. Its time dependence originates from the Higgs-inflaton/-curvature coupling [Eq. (2.5)]. The creation/annihilation operator $\hat{a}_{\mathbf{k}}$ satisfies the following algebras: $[\hat{a}_{\mathbf{k}}, \hat{a}_{\mathbf{k}'}^\dagger] = \delta(\mathbf{k} - \mathbf{k}')$ and $[\hat{a}_{\mathbf{k}}, \hat{a}_{\mathbf{k}'}] = [\hat{a}_{\mathbf{k}}^\dagger, \hat{a}_{\mathbf{k}'}^\dagger] = 0$. We can always take the initial conditions such that $h_{\mathbf{k}}(0) = 1/\sqrt{2\omega_{\mathbf{k};h}(0)}$ and $\dot{h}_{\mathbf{k}}(0) = -i\sqrt{\omega_{\mathbf{k};h}(0)}/2$ using the Bogolyubov transformation. Then, the initial vacuum state is annihilated by the corresponding annihilation operator $\hat{a}_{\mathbf{k}}$ as $\hat{a}_{\mathbf{k}}|0; \text{in}\rangle = 0$. Here we keep only the leading order WKB result with respect to the cosmic expansion. See App. A for more details.

One can discuss particle production by means of Bogolyubov coefficients using the above mode expansion as done in literature. Nevertheless, it is instructive to see the same physics in a different viewpoint, by only looking at correlators, since the relation with outcomes of classical lattice simulations can be seen clearly.^{∞8} We define two correlators and their Fourier transforms [43–47]:

$$\langle [h(x), h(y)]_+ \rangle \equiv \int_{\mathbf{k}} \frac{e^{i\mathbf{k}\cdot(\mathbf{x}-\mathbf{y})}}{[a(x_0)a(y_0)]^{3/2}} G_{F;h}(x_0, y_0; \mathbf{k}), \quad (2.9)$$

$$\langle [h(x), h(y)]_- \rangle \equiv \int_{\mathbf{k}} \frac{e^{i\mathbf{k}\cdot(\mathbf{x}-\mathbf{y})}}{[a(x_0)a(y_0)]^{3/2}} G_{\rho;h}(x_0, y_0; \mathbf{k}), \quad (2.10)$$

where $[\bullet, \bullet]_{\pm}$ stands for the anti-commutator/commutator respectively, expectation values $\langle \bullet \rangle$, are taken by the initial vacuum state, and we adopt the following shorthanded notation $\int_{\mathbf{k}} \equiv \int d^3k/(2\pi)^3$. These two propagators, $G_{F/\rho}$, are referred to as the statistical/spectral functions respectively. The statistical function encodes the occupation number and the

^{∞8} Also, it may be conceptually clear especially when the effects of inflaton/Higgs particle production becomes relevant, though it is equivalent after an appropriate reinterpretation.

spectral function reflects the spectrum of theory (*i.e.* location of poles for particle-like excitations and branch-cuts for continuum). They are expressed in terms of wave functions if one neglects interaction terms:

$$G_{F/\rho;h}(x_0, y_0; \mathbf{k}) = [h_{\mathbf{k}}(x_0)h_{\mathbf{k}}^*(y_0) \pm h_{\mathbf{k}}^*(x_0)h_{\mathbf{k}}(y_0)]. \quad (2.11)$$

In classical lattice simulations, which we discuss later, one can compute the left hand side of Eqs. (2.9) and (2.10) by regarding the field variables as classical ones. Note that there is no counterpart of the spectral function in classical lattice simulations, and indeed the classical approximations are justified only for $|G_F| \gg |G_\rho|$ [48]. By using G_F , we can define the expectation value of energy density $\langle \hat{T}^{00} \rangle$ as [49, 50]:

$$\langle \hat{T}_h^{00}(x) \rangle = \int_{\mathbf{k}/a(x_0)} \frac{1}{4} [\partial_{x_0} \partial_{y_0} + \omega_{k;h}^2(x_0)] G_{F;h}(x_0, y_0; \mathbf{k}) \Big|_{y_0 \rightarrow x_0} - (\text{Vac.}) + \dots \quad (2.12)$$

$$= \int_{\mathbf{k}/a(x_0)} \frac{1}{2} [|\dot{h}_{\mathbf{k}}(x_0)|^2 + \omega_{k;h}^2(x_0)|h_{\mathbf{k}}(x_0)|^2 - \omega_{k;h}(x_0)] + \dots. \quad (2.13)$$

Here, again, we only keep the leading order term in the WKB approximation with respect to the cosmic expansion. The term (Vac.) subtracts vacuum fluctuations. This motivates the following definition of the comoving number density in the momentum space:

$$n_{k;h}(t) = \frac{1}{2\omega_{k;h}(t)} [|\dot{h}_{\mathbf{k}}(t)|^2 + \omega_{k;h}^2(t)|h_{\mathbf{k}}(t)|^2] - \frac{1}{2}, \quad (2.14)$$

at the leading order in $H^2/\omega_{k;h}^2$ expansion. Note that the initial condition of the wave function $h_{\mathbf{k}}$ implies $n_{k;h}(0) = 0$. The physical energy and number densities are given by $\int_{\mathbf{k}/a(t)} \omega_{k;h} n_{k;h}$ and $\int_{\mathbf{k}/a(t)} n_{k;h}$, respectively.

The break-down of adiabaticity plays the key role in the following discussion. To see this, we take the time derivation of the number density of Higgs:

$$\dot{n}_{k;h} \sim \mathcal{O}(\dot{\omega}_{k;h}/\omega_{k;h}^2) \omega_{k;h} n_{k;h}. \quad (2.15)$$

Here we have used the equation of motion [Eq. (2.8)], and keep the leading order terms in $H^2/\omega_{k;h}^2$ expansion. Thus, the number density increases only if adiabaticity breaks down, *i.e.* $|\dot{\omega}_{k;h}/\omega_{k;h}^2| \gtrsim 1$. Indeed, the WKB solution of Eq. (2.8) $h_{\mathbf{k}}(t) = e^{-i \int^t d\tau \omega_{k;h}(\tau)} / \sqrt{2\omega_{k;h}(t)}$, which is valid for the adiabatic region $|\dot{\omega}_{k;h}/\omega_{k;h}^2| \ll 1$, leaves the number density unchanged from that of vacuum up to corrections of $\mathcal{O}(|\dot{\omega}_{k;h}/\omega_{k;h}^2|)$.^{∞9} Thus, the Higgs field acquires fluctuations for the non-adiabatic change of $\omega_{k;h}(t)$ induced by the Higgs-inflaton/-curvature coupling [Eq. (2.5)].^{∞10}

^{∞9} The narrow resonance may be regarded as particle production proportional to this small number, $|\dot{\omega}_{k;h}/\omega_{k;h}^2| \ll 1$.

^{∞10} At the onset of inflaton oscillation, Higgs fluctuations are also produced because the Hubble parameter changes non-adiabatically [51] except for the conformal coupling $\xi = 1/6$. However, the inflaton oscillation provides more violent production of Higgs fluctuations as we will see.

2.1 Preheating via quartic stabilization: $c^2\phi^2h^2$

Qualitative discussion

First let us consider the Higgs-inflaton quartic coupling case. In this case, the dispersion relation of Higgs is given by

$$\omega_{k;h}^2(t) = c^2\Phi^2(t)\cos^2(m_\phi t) + \frac{k^2}{a^2(t)} + \delta m_{\text{self};h}^2(t) \quad (2.16)$$

where $\delta m_{\text{self};h}^2$ represents a finite density correction to the Higgs mass term from the Higgs self interaction, which we discuss later. At first $\delta m_{\text{self};h}^2$ can be neglected since there are no Higgs particles right after the inflation. Utilizing the conventional parameterization,

$$q(t) = \frac{c^2\Phi^2(t)}{4m_\phi^2}, \quad A_k(t) = \frac{k^2}{m_\phi^2 a^2(t)} + \frac{c^2\Phi^2(t)}{2m_\phi^2}, \quad (2.17)$$

we can reorganize the equation of motion [Eq. (2.8)] as follows

$$\left[\frac{d^2}{d(m_\phi t)^2} + A_k(t) - 2q(t)\cos(2m_\phi t) \right] h_k(t) = 0. \quad (2.18)$$

Here again we keep leading terms in $H^2/\omega_{k;h}^2$ expansion. If one neglects the cosmic expansion, namely for constant q and A_k , it is nothing but the Mathieu equation. Depending on parameters q and A_k , the wave function grows exponentially or oscillates with a constant amplitude.

From now we focus on the effect of inflaton oscillation on the adiabaticity of Higgs. Note that the cosmic expansion can be treated adiabatically, *i.e.* $m_\phi \gg H^{\heartsuit 11}$ after several oscillations of inflaton, and hence we do not consider its effect on the adiabaticity of Higgs. Let us quantify when the inflaton oscillation becomes non-adiabatic for the Higgs by using the condition $|\dot{\omega}_{k;h}/\omega_{k;h}^2| > 1$. The left-hand-side tends to become large when the inflaton passes through $\phi \sim 0$ because the denominator gets smaller. Around $\phi \sim 0$, one can estimate

$$\left| \frac{\dot{\omega}_{k;h}}{\omega_{k;h}^2} \right| \sim \left| \frac{c^2\Phi^2 m_\phi^2 t}{(k^2/a^2 + c^2\Phi^2 m_\phi^2 t^2)^{3/2}} \right| \lesssim \frac{c\Phi m_\phi}{k^2/a^2}. \quad (2.19)$$

The second inequality is saturated if one inserts $t \sim k/a/c\Phi m_\phi$. If $m_\phi \gg c\Phi$ (*i.e.* $q \ll 1$), Higgs is produced within narrow bands $k/a \sim m_\phi(1 \pm q)$. $m_\phi \gg c\Phi$ ensures the adiabaticity is not broken down. Since Higgs is boson, induced emission effects of previously produced Higgs could make the dynamics non-perturbative (*i.e.* narrow resonance [27–29]), but usually the cosmic expansion soon kills such a resonant amplification.^{\heartsuit 12} Hence, the produced amount of Higgs fluctuations during the narrow resonance is not so significant. On the other hand, for $m_\phi < c\Phi$ (*i.e.* $q > 1$), the bands get broad, and the adiabaticity is badly broken down for modes with $k^2/a^2 \lesssim c\Phi m_\phi$. This is the sign of non-perturbative Higgs production [25, 26]. To sum up, the Higgs fluctuations with $k/a \lesssim p_*$ are efficiently produced if the following inequality holds:

$$p_*(t) \gtrsim m_\phi; \quad p_*(t) \equiv \sqrt{c m_\phi \Phi(t)}, \quad (2.20)$$

^{\heartsuit 11} Strictly speaking, a small oscillating term remains in the scale factor a [52].

^{\heartsuit 12} The modes within the resonant band are efficiently red-shifted away if $q^2 m_\phi < H$. If this condition fulfills, the narrow resonance does not take place. Since we are mainly interested in the very early stage of preheating after chaotic inflation, we expect $H \sim m_\phi$. One can see that $q^2 m_\phi < H$ tends to be satisfied for $q \ll 1$.

where $p_*(=k_*/a)$ is a characteristic physical momentum of Higgs particle production.

We assume that this inequality is satisfied at the onset of the inflaton oscillation in the following discussion. It indicates that the quartic coupling should satisfy $c\Phi_{\text{ini}} > m_\phi$, or

$$c > 4 \times 10^{-6} \left[\frac{m_\phi}{1.5 \times 10^{13} \text{ GeV}} \right] \left[\frac{\sqrt{2} M_{\text{pl}}}{\Phi_{\text{ini}}} \right], \quad (2.21)$$

where Φ_{ini} is the initial inflaton amplitude. This inequality implies $c\Phi_{\text{ini}} > H_{\text{inf}}$, with H_{inf} being the Hubble scale at the end of inflation, since $m_\phi \gtrsim H_{\text{inf}}$ holds generically. Thus the stabilization of the Higgs field during inflation is ensured under the assumption (2.20).¹³ Hereafter we consider this situation.

The Higgs mode whose momentum is below p_* acquires fluctuations for each passage of $\phi \sim 0$, and its mode function becomes $h_k(t) = [\alpha_k(t)e^{-i \int^t \omega_{k;h}} + \beta_k(t)e^{i \int^t \omega_{k;h}}] / \sqrt{2\omega_{k;h}(t)}$ outside the region in which the adiabaticity of Higgs is broken down. Here α_k and β_k are the Bogolyubov coefficients, satisfying $|\alpha_k|^2 - |\beta_k|^2 = 1$. As explained below Eq. (2.15), Higgs fluctuations are not produced for $|\alpha_k| = 1$ and $\beta_k = 0$. A non-zero value of β_k indicates the Higgs production. After several times of the passages of $\phi \sim 0$, its number density grows exponentially due to the Bose enhancement [25, 26]:

$$n_h(t) = \int_{\mathbf{k}/a(t)} n_{k;h}(t) = \int_{\mathbf{k}/a(t)} |\beta_k(t)|^2 \simeq \int_{\mathbf{k}/a(t)} \frac{e^{2\mu_k m_\phi t}}{2} \quad (2.22)$$

$$\sim \frac{1}{32\pi^2} \sqrt{\frac{\pi}{2\mu_{\text{qtc}} m_\phi t}} e^{2\mu_{\text{qtc}} m_\phi t} p_*^3(t), \quad (2.23)$$

where μ_k is a momentum dependent function, and it has a maximum value $\mu_{\text{qtc}} \simeq \mathcal{O}(0.1)$ at $k \simeq k_*/2$. Here we have used the steepest descent method to evaluate the integral, and estimated the second derivative of μ_k as $\mu''_{k_*} \sim 2\mu_{\text{qtc}}/\delta k^2$ with $\delta k \sim k_*/2$.

While the Higgs fluctuation continuously grows, it induces effective mass corrections to inflaton and Higgs itself via the quartic interaction, $c^2\phi^2 h^2$, and the self interaction, λh^4 , respectively. In our case, the self coupling λ is larger than c^2 , and hence we just consider the latter effect. The self coupling λ is negative in the case of our interest at least for $m_\phi > h_{\text{max}}$, which is fulfilled for the center value of the top quark mass [See also the discussion below Eq. (2.5)]. Therefore, the self coupling induces the tachyonic mass term:

$$\begin{aligned} \delta m_{\text{self};h}^2(t) &= -3\tilde{\lambda} \int_{\mathbf{k}/a(t)} \frac{1}{2} G_{F;h}(t, t; \mathbf{k}) = -3\tilde{\lambda} \int_{\mathbf{k}/a(t)} |h_k(t)|^2 \\ &\simeq -3\tilde{\lambda} \int_{\mathbf{k}/a(t)} \frac{n_{k;h}(t)}{\omega_{k;h}(t)} \\ &\sim -3\tilde{\lambda} \frac{n_h(t)}{\omega_{k_*;h}(t)}. \end{aligned} \quad (2.24)$$

This term forces the Higgs field to roll down to its true minimum.

Now let us derive the condition when Higgs rolls down to the true vacuum. One might estimate it by simply comparing the effective masses induced by the Higgs-inflaton coupling and the self coupling as $|\delta m_{\text{self};h}^2| \gtrsim c^2\Phi^2$, *but this is not correct*. The important point here is

¹³ If there is a hierarchy $m_\phi \gg H_{\text{inf}}$ (or $\Phi_{\text{ini}} \ll M_{\text{pl}}$), it is possible to choose $H_{\text{inf}} < c\Phi_{\text{ini}} < m_\phi$. In such a case, the Higgs field is stabilized during inflation and also there is no violent Higgs production after inflation.

that the effective mass induced by the Higgs-inflaton coupling is oscillating, and hence Higgs infrared modes is tachyonic for some small time interval at around when ϕ crosses the origin even if $|\delta m_{\text{self},h}^2| \ll c^2 \Phi^2$.^{♥14} The time interval Δt during which the inflaton-induced Higgs effective mass is negligible compared to $\delta m_{\text{self},h}^2$ is estimated as

$$m_\phi^2 q(m_\phi \Delta t)^2 \sim |\delta m_{\text{self},h}^2|, \quad (2.25)$$

where $\phi \sim \Phi m_\phi \Delta t$ at around the potential origin. During this time interval, the tachyonic effective mass, $\delta m_{\text{self},h}$, can make the Higgs field grow. The growth rate of the Higgs field during this time interval is estimated as $|\delta m_{\text{self},h}| \Delta t \sim |\delta m_{\text{self},h}^2| / p_*^2$. If it exceeds unity, the Higgs field increases by a large amount due to the tachyonic effective mass, $\delta m_{\text{self},h}$, and it escapes from the metastable electroweak vacuum. Thus, the following inequality should be satisfied for the electroweak vacuum not to decay:

$$\left| \delta m_{\text{self},h}^2(t) \right|_{\phi \sim 0} \lesssim p_*^2(t) \leftrightarrow \frac{3\tilde{\lambda}}{16\pi^2} \sqrt{\frac{\pi}{2\mu_{\text{qtc}} m_\phi t}} e^{2\mu_{\text{qtc}} m_\phi t} \lesssim 1, \quad (2.26)$$

where the subscript $\phi \sim 0$ indicates that the effective mass is evaluated at the passage of $\phi \sim 0$. Interestingly, the left inequality suggests that not only the long wave length mode of Higgs but all the modes below p_* overcomes the pressure due to the tachyonic effective mass if this inequality is violated. Hence, the transition is expected to be dominated by the scale below p_* .

Eq. (2.26) implies that the electroweak vacuum decays at^{♥15}

$$t_{\text{dec}} \sim \frac{1}{2\mu_{\text{qtc}} m_\phi} \ln \left(\frac{16\pi^{\frac{3}{2}}}{3\tilde{\lambda}} \right). \quad (2.27)$$

Before this time, the non-perturbative Higgs production should shut off due to the cosmic expansion for the electroweak vacuum to survive the preheating stage. The cosmic expansion kills the non-perturbative Higgs production at $p_*(t_{\text{end}}) \sim m_\phi$,^{♥16} which implies

$$t_{\text{end}} \sim \frac{2\sqrt{6}}{3m_\phi} \frac{c M_{\text{pl}}}{m_\phi}. \quad (2.28)$$

Therefore, the electroweak vacuum survives the preheating stage for $t_{\text{end}} \lesssim t_{\text{dec}}$, which yields the following upper bound for the Higgs-inflaton coupling:

$$c \lesssim \frac{\sqrt{6}}{8\mu_{\text{qtc}}} \frac{m_\phi}{M_{\text{pl}}} \ln \left(\frac{16\pi^{\frac{3}{2}}}{3\tilde{\lambda}} \right) \simeq 10^{-4} \left[\frac{0.1}{\mu_{\text{qtc}}} \right] \left[\frac{m_\phi}{10^{13} \text{ GeV}} \right]. \quad (2.29)$$

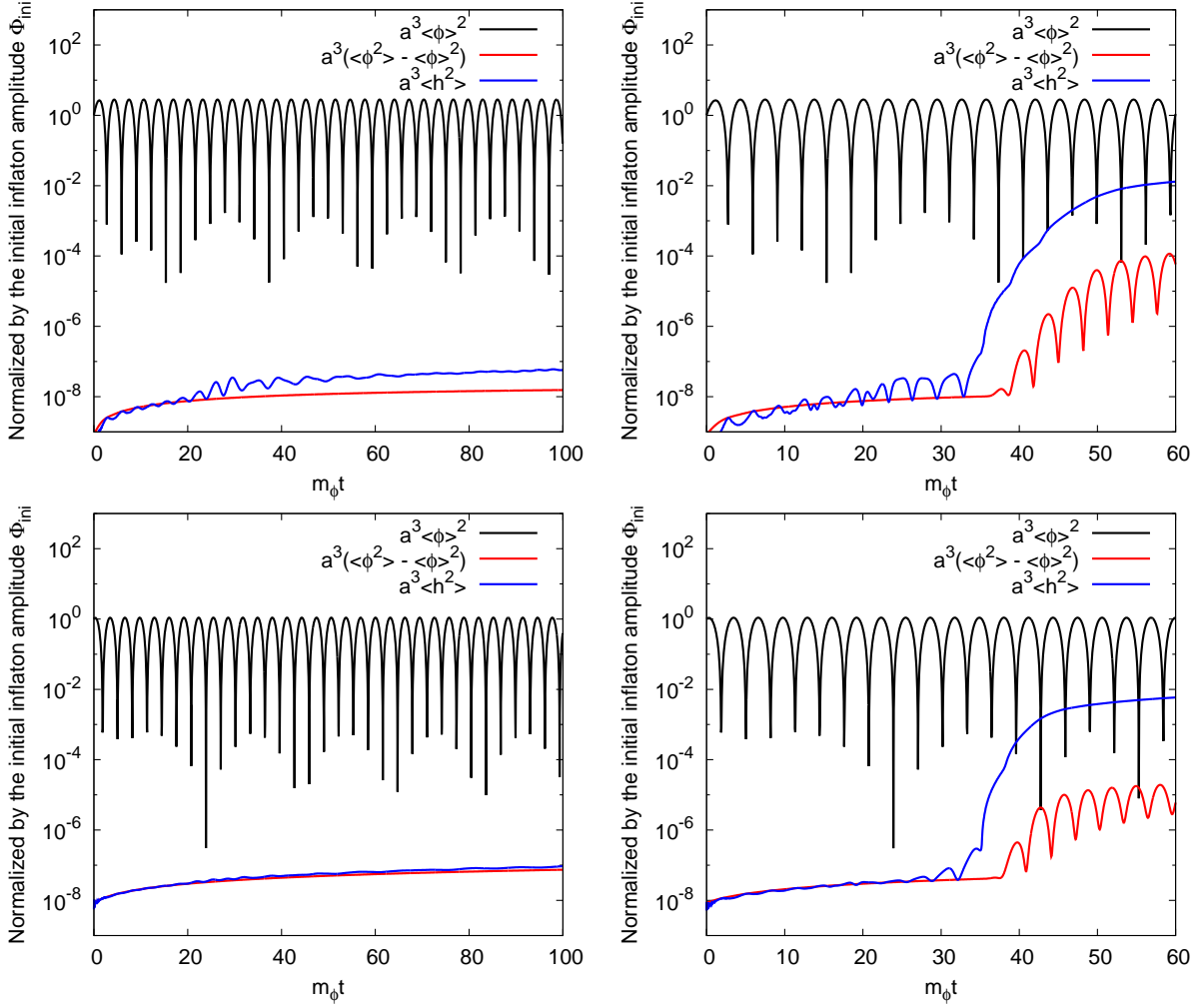


Figure 1: Numerical calculation of the time evolution of the inflaton expectation value (black), the inflaton dispersion (red) and the Higgs dispersion (blue). We take the parameters as $N = 128^3$, $dt = 10^{-3}/m_\phi$, $L = 10/m_\phi$ and $m_\phi = 1.5 \times 10^{13}$ GeV. Upper left panel: $c = 1 \times 10^{-4}$ and $\Phi_{\text{ini}} = \sqrt{2} M_{\text{pl}}$. Upper right panel: $c = 2 \times 10^{-4}$ and $\Phi_{\text{ini}} = \sqrt{2} M_{\text{pl}}$. Lower left panel: $c = 1 \times 10^{-4}$ and $\Phi_{\text{ini}} = \sqrt{0.2} M_{\text{pl}}$. Lower right panel: $c = 2 \times 10^{-4}$ and $\Phi_{\text{ini}} = \sqrt{0.2} M_{\text{pl}}$. Higgs remains in the electroweak vacuum in the left panels, while it rolls down to the true vacuum in the right panels.

Numerical simulation

Below, we show the results of 3+1-dimensional classical lattice simulations for the quartic coupling case. The main purpose here is to confirm the upper bound given in Eq. (2.29).

¹⁴ In other words, we cannot take the oscillation average if the time scale of our interest, $\delta m_{\text{self},h}$, is faster than the oscillation period, $m_\phi^2 < |\delta m_{\text{self},h}^2|$, which is the case we have to deal with in order to estimate the upper bound on c .

¹⁵ If h_{max} is sufficiently large, say $h_{\text{max}} \gg (q/\tilde{\lambda}^2)^{1/4} m_\phi$, t_{dec} corresponds to the time at which the resonance shuts off due to the positive Higgs quartic coupling. Here we assume h_{max} is quite small: $h_{\text{max}} \simeq 10^{10}$ GeV.

¹⁶ Strictly speaking, after the broad resonance, a narrow resonance takes place, but it is soon killed by the cosmic expansion at $q^2 m_\phi \simeq H$.

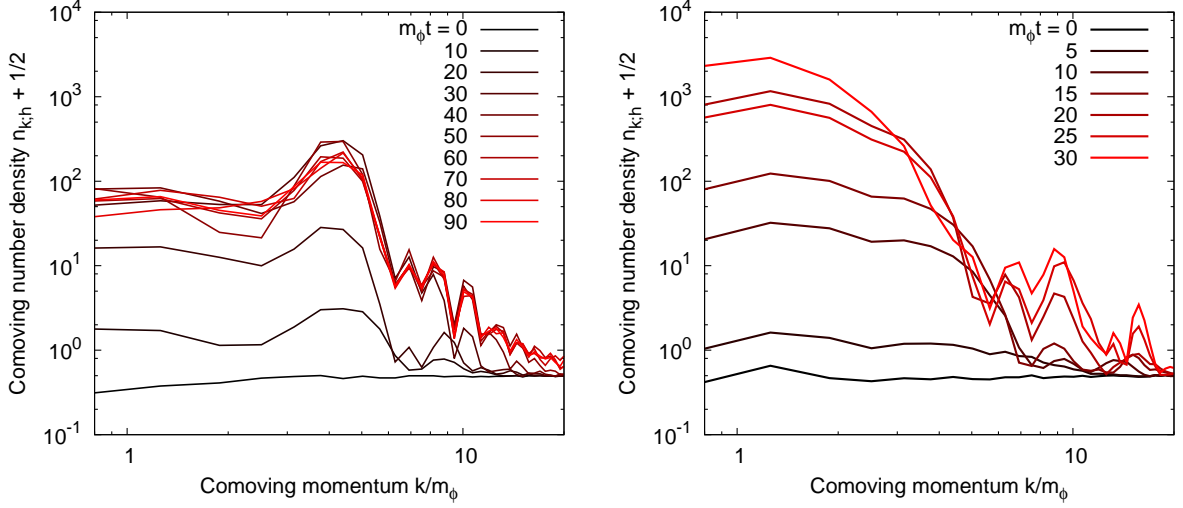


Figure 2: Time evolution of the comoving number density of Higgs. We take the parameters as $N = 128^3$, $dt = 10^{-3}/m_\phi$, $L = 10/m_\phi$, $m_\phi = 1.5 \times 10^{13}$ GeV and $\Phi_{\text{ini}} = \sqrt{2} M_{\text{pl}}$. Left panel: $c = 1 \times 10^{-4}$. Right panel: $c = 2 \times 10^{-4}$.

We solve the following classical equations of motion in the configuration space:

$$0 = \ddot{\phi} + 3H\dot{\phi} - \frac{1}{a^2} \partial_i^2 \phi + (m_\phi^2 + c^2 h^2) \phi, \quad (2.30)$$

$$0 = \ddot{h} + 3H\dot{h} - \frac{1}{a^2} \partial_i^2 h + (c^2 \phi^2 + \lambda h^2) h, \quad (2.31)$$

for the scalar fields, and

$$H^2 = \frac{\langle \rho \rangle}{3M_{\text{pl}}^2}, \quad (2.32)$$

for the metric, where the total energy density is given by

$$\rho = \frac{1}{2} \left(\dot{\phi}^2 + \frac{1}{a^2} (\partial_i \phi)^2 + m_\phi^2 \phi^2 \right) + \frac{1}{2} \left(\dot{h}^2 + \frac{1}{a^2} (\partial_i h)^2 \right) + \frac{\lambda}{4} h^4 + \frac{1}{2} c^2 \phi^2 h^2, \quad (2.33)$$

and $\langle \dots \rangle$ denotes the spatial average. We neglect fluctuations of the metric because their effects are suppressed by the Planck mass. The grid number is taken as $N = 128^3$ with a comoving edge size being $L = 10/m_\phi$ and the time step is $dt = 10^{-3}/m_\phi$. The inflaton mass is fixed as $m_\phi = 1.5 \times 10^{13}$ GeV. We show results for $c = 1 \times 10^{-4}$ and $c = 2 \times 10^{-4}$. Some details of our numerical calculation are summarized below.^{♡17}

- We solve the classical equations of motion with the initial inflaton amplitude $\Phi_{\text{ini}} = \sqrt{2} M_{\text{pl}}$ or $\sqrt{0.2} M_{\text{pl}}$. By changing Φ_{ini} , we test whether or not the inflation scale changes the bounds on the coupling strength. We take the initial velocity as $\dot{\Phi}_{\text{ini}} = 0$, but we have checked that our results are insensitive to this choice. We also introduce gaussian initial fluctuations on the inflaton and Higgs field following Refs. [54, 55], which mimic the quantum vacuum fluctuations.
- We renormalize masses of inflaton and Higgs originating from the initial quantum fluctuations. See App. B for more details on this procedure.

^{♡17} We have also confirmed our results by using LATTICEASY [53].

- There is another equation of motion for the metric sector, and it is redundant. We have checked that our numerical calculation satisfies the redundancy at least at $\mathcal{O}(10^{-3})$ precision.
- In order to avoid numerical divergence, we add a sextic term to the Higgs potential. We take the coefficient of the sextic term such that the Higgs field value h_{\min} at the true minimum is $\tilde{\lambda} h_{\min}^2 = 5 \times 10^{-8} M_{\text{pl}}^2$. The inequality $\tilde{\lambda} h_{\min}^2 \gg c^2 \Phi^2$ is satisfied at the time when Higgs rolls down to the true vacuum, and hence the sextic term does not affect the Higgs dynamics before the electroweak vacuum decay. We have verified that it is not affected whether or not the electroweak vacuum decays by the sextic term, by changing the coefficient of it.

In Fig. 1, we show the time evolution of the inflaton vacuum expectation value squared $\langle \phi \rangle^2$ (black), the inflaton dispersion $\langle \phi^2 \rangle - \langle \phi \rangle^2$ (red) and the Higgs dispersion $\langle h^2 \rangle$ (blue). Here $\langle \bullet^2 \rangle$ corresponds to $\langle [\bullet, \bullet]_+ \rangle / 2$, and thus can be expressed by the statistical function, $G_{E, \bullet}$. See Eq. (2.9). They are multiplied by the scale factor to the third, where the initial scale factor is taken as $a_{\text{ini}} = 1$. We take the coupling as $c = 1 \times 10^{-4}$ for the left panels and $c = 2 \times 10^{-4}$ for the right panels, respectively. The initial inflaton amplitudes are $\Phi_{\text{ini}} = \sqrt{2} M_{\text{pl}}$ for the upper panels and $\Phi_{\text{ini}} = \sqrt{0.2} M_{\text{pl}}$ for the lower panels.

As it is clear from Fig. 1, Higgs stays at the electroweak vacuum for $c = 1 \times 10^{-4}$, while it rolls down to the true vacuum for $c = 2 \times 10^{-4}$, independent of the initial inflaton amplitude. It is consistent with our estimation (2.29). In fact, an interesting feature of Eq. (2.29) is that it does not depend on the initial inflaton amplitude or the inflation scale as long as the inequality (2.20) is satisfied initially. This is because the growth rate, $\mu_{\text{qt},c}$, does not much depend on the inflaton amplitude for the broad resonance.^{♡18} Thus, the Higgs fluctuations are efficiently produced at the latest epoch [Eq. (2.28)] independent of the initial inflaton amplitude, since the number of the inflaton oscillation is dominated by that epoch.

We also plot the time evolution of the comoving number density of Higgs [Eq. (2.14)] for $\Phi_{\text{ini}} = \sqrt{2} M_{\text{pl}}$ in Fig. 2. The left panel shows the case with $c = 1 \times 10^{-4}$ and the right panel does the case with $c = 2 \times 10^{-4}$. In the left panel, Higgs is efficiently produced at the beginning of the oscillation, but the resonance shuts off due to the Hubble expansion. After $t \simeq 30/m_\phi$, the comoving number density of Higgs remains almost constant. On the other hand, in the right panel, the comoving number density of Higgs continues to grow resonantly.^{♡19} As a result, Higgs rolls down to the true vacuum once the condition (2.26) is satisfied. Also, one can see that modes below p_* is efficiently produced as expected. The time evolution of the number density for $\Phi_{\text{ini}} = \sqrt{0.2} M_{\text{pl}}$ is quite similar.

2.2 Preheating via curvature stabilization: $\xi R h^2$

Qualitative discussion

Next, let us consider the Higgs-curvature coupling case. In this case, the dispersion relation of Higgs is given by

$$\omega_{k;h}^2(t) = \xi R + \frac{\mathbf{k}^2}{a^2(t)} + \delta m_{\text{self};h}^2(t), \quad (2.34)$$

^{♡18} As we will see later, the situation is completely different for the Higgs-curvature coupling case.

^{♡19} We do not plot the comoving number density of Higgs for $m_\phi t > 30$ in the right panel because Higgs already rolls down to the true vacuum before that time.

with the Ricci scalar being $R = 6[\ddot{a}/a + (\dot{a}/a)^2]$. In the inflaton-oscillation dominated era, the scale factor satisfies the following equalities:

$$\left[\frac{\dot{a}(t)}{a(t)}\right]^2 = \frac{1}{6M_{\text{pl}}^2} \left[\dot{\phi}^2(t) + m_\phi^2 \phi^2(t)\right], \quad \frac{\ddot{a}(t)}{a(t)} = \frac{1}{3M_{\text{pl}}^2} \left[\frac{1}{2}m_\phi^2 \phi^2(t) - \dot{\phi}^2(t)\right]. \quad (2.35)$$

Plugging Eqs. (2.6) and (2.35) into the dispersion relation, we get

$$\omega_{k;h}^2(t) + \Delta(t) \simeq \frac{3}{2} \left(\xi - \frac{1}{4}\right) \frac{m_\phi^2}{M_{\text{pl}}^2} \Phi^2(t) \cos(2m_\phi t) + \left[\frac{k^2}{a^2(t)} + \frac{\xi m_\phi^2}{2M_{\text{pl}}^2} \Phi^2(t)\right] + \delta m_{\text{self};h}^2(t). \quad (2.36)$$

In contrast to the case of the quartic interaction [Eq. (2.16)], the modes can be tachyonic in one oscillation when ξ satisfies $\xi < 3/16$ or $3/8 < \xi$. Otherwise they are stable. If $\xi \Phi^2/M_{\text{pl}}^2 < \mathcal{O}(1)$, the production becomes indistinguishable from the narrow resonance.^{♡20} Thus, we concentrate on the case with^{♡21}

$$\xi > \left[\frac{\sqrt{2}M_{\text{pl}}}{\Phi_{\text{ini}}}\right]^2, \quad (2.37)$$

where an efficient particle production via the tachyonic instability occurs, which we call tachyonic resonance. Note that if this inequality holds, the Higgs stability during inflation is ensured since $\Phi_{\text{ini}} \lesssim M_{\text{pl}}$ leads to $\xi \gtrsim \mathcal{O}(1)$.^{♡22} In this case, the growth rate of the number density $X_k(t)$ is estimated as [56]:^{♡23}

$$X_k(t) \simeq -\frac{x}{\sqrt{q}} A_k + 2x\sqrt{q}, \quad (2.38)$$

where

$$q(t) = \frac{3}{4} \left(\xi - \frac{1}{4}\right) \frac{\Phi^2(t)}{M_{\text{pl}}^2}, \quad A_k(t) = \frac{k^2}{a^2(t)m_\phi^2} + \frac{\xi \Phi^2(t)}{2M_{\text{pl}}^2}, \quad (2.39)$$

with $x \simeq 0.85$. Recalling that $\Phi(t) \propto 1/t$, one can see that the first few oscillations play the dominant role in the tachyonic resonance. The growth rate is rather power law like, contrary to the exponential growth in the previous case. The typical physical momentum enhanced by the tachyonic resonance is given by

$$p_*^{(\text{tac})}(t) \equiv \frac{1}{\sqrt{x}} m_\phi q^{1/4}(t). \quad (2.40)$$

In terms of $p_*^{(\text{tac})}$, the condition for the efficient particle production via the tachyonic preheating has the similar expression as Eq. (2.20):

$$p_*^{(\text{tac})}(t) \gtrsim m_\phi. \quad (2.41)$$

^{♡20} In fact, it is almost stable for $\xi \Phi^2/M_{\text{pl}}^2, \Phi^2/M_{\text{pl}}^2 < 1$. See Ref. [31].

^{♡21} We do not consider the case with $-\xi \gtrsim \mathcal{O}(1)$ because the Higgs-curvature coupling does not stabilize the electroweak vacuum during inflation.

^{♡22} If $\Phi_{\text{ini}} \ll M_{\text{pl}}$, it is possible to choose $\mathcal{O}(0.1) < \xi < (M_{\text{pl}}/\Phi_{\text{ini}})^2$. In such a case, Higgs is stable during inflation and also tachyonic resonance does not occur after inflation.

^{♡23} This is understood as follows. The time interval during which the Higgs with momentum $p = k/a$ becomes tachyonic in one inflaton oscillation is $\Delta t_k \sim m_\phi^{-1}(1 - p^2/\xi R)$ for $p^2 \lesssim \xi R$ (here R should be regarded as just a typical value). In one inflaton oscillation, these modes are enhanced as $\exp(\sqrt{\xi R} \Delta t_k) \sim \exp(\sqrt{q} - p^2/p_*^{(\text{tac})2}) \sim \exp(\sqrt{q} - A_k/\sqrt{q})$, where $p_*^{(\text{tac})}$ is defined in (2.40).

The number density of Higgs field produced after the j -th passage of $\phi \sim 0$ is estimated as

$$n_h(t_j) = \int_{k/a(t_j)} n_{k;h}(t_j) \simeq \int_{k/a(t_j)} e^{2\sum_{i=1}^j X_k(t_i)} \sim \frac{1}{16\pi^2} \sqrt{\frac{\pi}{2}} e^{n_{\text{eff}}(t_j)\mu_{\text{crv}}\sqrt{\xi}\frac{\Phi_{\text{ini}}}{M_{\text{pl}}}} \frac{a^3(t_{\text{ini}})}{a^3(t_j)} p_*^{(\text{tac})^3}(t_{\text{ini}}), \quad (2.42)$$

where $\mu_{\text{crv}} \simeq 2x\sqrt{4/3} \simeq 2$ for $\xi \gtrsim \mathcal{O}(1)$, and Φ_{ini} is the initial inflaton amplitude. The effective number of times of oscillation, $n_{\text{eff}}(t_j) \equiv \sum_{i=1}^j \Phi(t_i)/\Phi_{\text{ini}}$, is a slightly time dependent function, which grows logarithmically. We estimate $n_{\text{eff}} \simeq 1$ for $\Phi_{\text{ini}} \gtrsim M_{\text{pl}}$. This is because the amplitude drastically decreases within the first oscillation, and hence the first one or two oscillations dominate the Higgs production. On the other hand, for $\Phi_{\text{ini}} \lesssim M_{\text{pl}}$, the later oscillations can also be important since the decrease of the amplitude is rather slow. For $\Phi_{\text{ini}} = \sqrt{0.2}M_{\text{pl}}$, for example, we roughly estimate $n_{\text{eff}} \simeq 1.5$ -2.

Now we are in a position to derive the condition where the electroweak vacuum is stable during the preheating. Contrary to the quartic stabilization, the curvature coupling becomes tachyonic every crossing around $\phi \sim 0$. Its time scale is of the order of m_ϕ^{-1} . During that period, the Higgs field grows towards an unwanted deeper minimum owing to the tachyonic mass terms from the curvature coupling $|\xi R|_{\phi \sim 0} \sim qm_\phi^2$ or the Higgs self coupling $|\delta m_{\text{self};h}^2|$. While the curvature coupling dominates the tachyonic mass, the growth rate of the Higgs field is estimated as $\sqrt{|\xi R|_{\phi \sim 0}}\Delta t \sim \sqrt{q}$. This is nothing but the efficiency of the resonance. Once that from the Higgs four point couplings becomes larger, the growth rate of the Higgs field is accelerated; $|\delta m_{\text{self};h}^2| \gtrsim qm_\phi^2$. Almost at the same time, the tachyonic mass term from the Higgs self coupling, $\delta m_{\text{self};h}^2$, exceeds the positive effective mass from the curvature coupling, $\xi R_{\phi \sim \Phi} \sim qm_\phi^2$, and the vacuum decay is triggered. Thus, we estimate the condition where Higgs is stable against the tachyonic mass as

$$\left| \delta m_{\text{self};h}^2(t_j) \right|_{\xi R \sim 0} \lesssim qm_\phi^2 \leftrightarrow \frac{3\tilde{\lambda}}{16\pi^2} \sqrt{\frac{\pi}{2q(t_{\text{ini}})}} \frac{a(t_{\text{end}})}{a(t_{\text{ini}})} e^{n_{\text{eff}}(t_{\text{end}})\mu_{\text{crv}}\sqrt{\xi}\frac{\Phi_{\text{ini}}}{M_{\text{pl}}}} \lesssim 1. \quad (2.43)$$

Again, one can see that not only the long wave length mode but all the modes below $q^{1/2}m_\phi$ grows towards the lower potential energy regime, overcoming the pressure of spatial gradients, if this condition is violated. As a result, the electroweak vacuum survives the tachyonic resonance for

$$\xi \lesssim \frac{1}{n_{\text{eff}}^2 \mu_{\text{crv}}^2} \left[\frac{M_{\text{pl}}}{\Phi_{\text{ini}}} \right]^2 \left[\ln \left(\frac{16\pi^2}{3\tilde{\lambda}} \sqrt{\frac{2}{\pi}} \right) \right]^2 \simeq 10 \left[\frac{2}{n_{\text{eff}} \mu_{\text{crv}}} \right]^2 \left[\frac{\sqrt{2}M_{\text{pl}}}{\Phi_{\text{ini}}} \right]^2, \quad (2.44)$$

where we have taken $q \simeq 1$ in the logarithm and neglect the scale factor dependence. This is because q cannot be much larger than $\mathcal{O}(1)$ in the present case since otherwise the tachyonic growth is catastrophic.

Here let us clarify differences of our analysis from that of Ref. [32], in which a similar study is performed for the Higgs-curvature coupling case. There are two main differences. First, the criteria for the Higgs field to escape from the electroweak vacuum is different. The authors in Ref. [32] compare the Higgs dispersion for the over-horizon modes $\sqrt{\langle h^2 \rangle_{aH}}$ and h_{max} (Λ_I in their notation). Instead, we take into account the stabilization effect from the

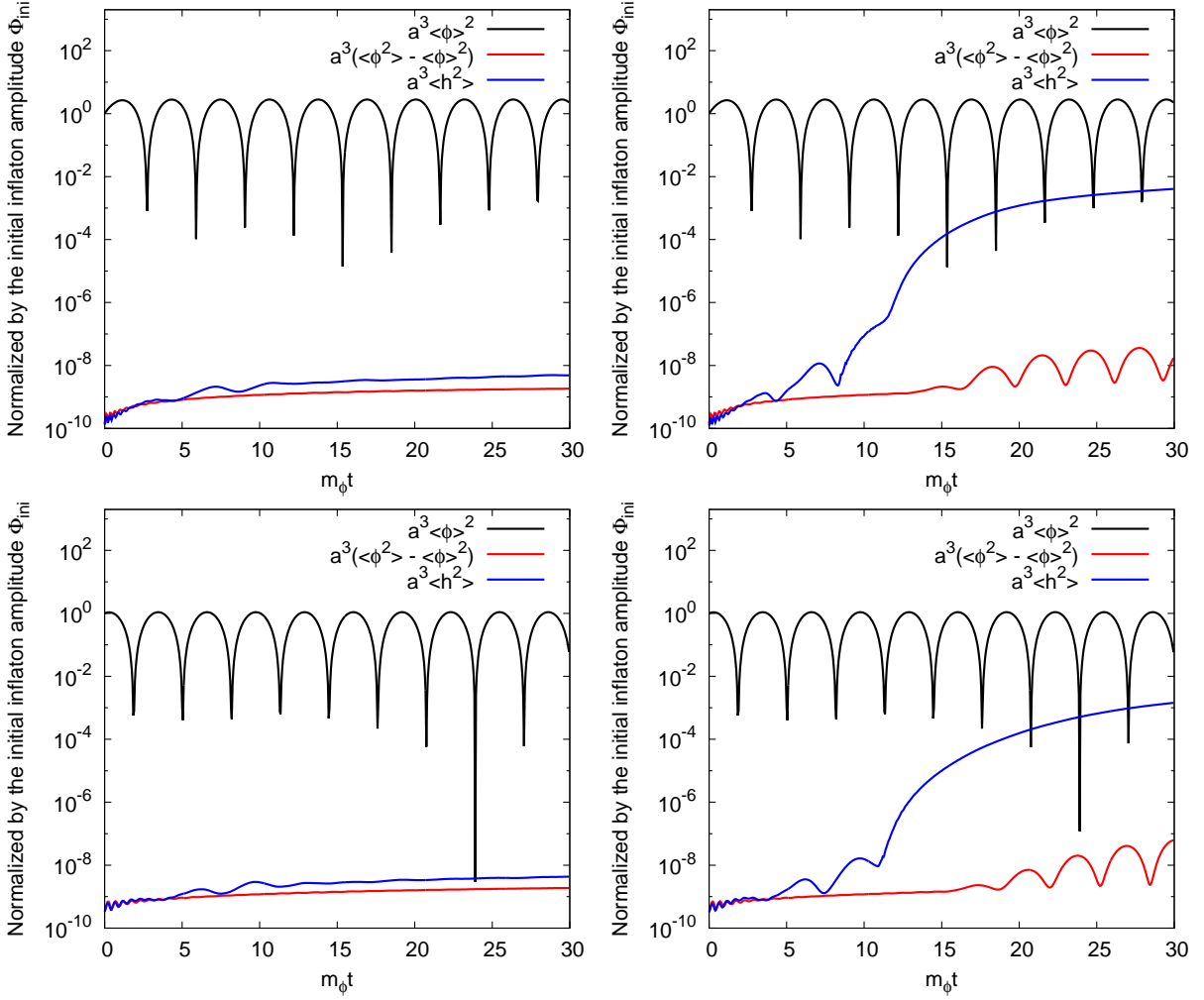


Figure 3: Numerical calculation of the time evolution of the inflaton expectation value (black), the inflaton dispersion (red) and the Higgs dispersion (blue). We take the parameters as $N = 128^3$, $dt = 10^{-3}/m_\phi$ and $m_\phi = 1.5 \times 10^{13}$ GeV. The comoving edge size is $L = 20/m_\phi$ for $\Phi_{\text{ini}} = \sqrt{2} M_{\text{pl}}$ and $L = 40/m_\phi$ for $\Phi_{\text{ini}} = \sqrt{0.2} M_{\text{pl}}$. Upper left panel: $\xi = 10$ and $\Phi_{\text{ini}} = \sqrt{2} M_{\text{pl}}$. Upper right panel: $\xi = 20$ and $\Phi_{\text{ini}} = \sqrt{2} M_{\text{pl}}$. Lower left panel: $\xi = 20$ and $\Phi_{\text{ini}} = \sqrt{0.2} M_{\text{pl}}$. Lower right panel: $\xi = 30$ and $\Phi_{\text{ini}} = \sqrt{0.2} M_{\text{pl}}$. Higgs remains in the electroweak vacuum in the left panels, while it rolls down to the true vacuum in the right panels.

Higgs-curvature coupling. We compare the effective masses induced by the Higgs self coupling and the Higgs-curvature coupling. Thus, the bound we obtain here is a bit weaker than their result. For definiteness, we perform a classical lattice simulation and confirm our estimation in the next section. Second, the treatment of the Higgs production caused by the Higgs-curvature coupling is also different. They treated the particle production caused by a transition of the mean-value of the Ricci scalar R after inflation [51] and the oscillation of R around the mean-value separately as a rough approximation. In our analysis, these effects are simultaneously included in the classical lattice simulation as we shall see below.

Numerical simulation

In the following, we show the results of classical lattice simulations for the curvature coupling case. The main purpose of this sub-section is to confirm the upper bound given in Eq. (2.44).

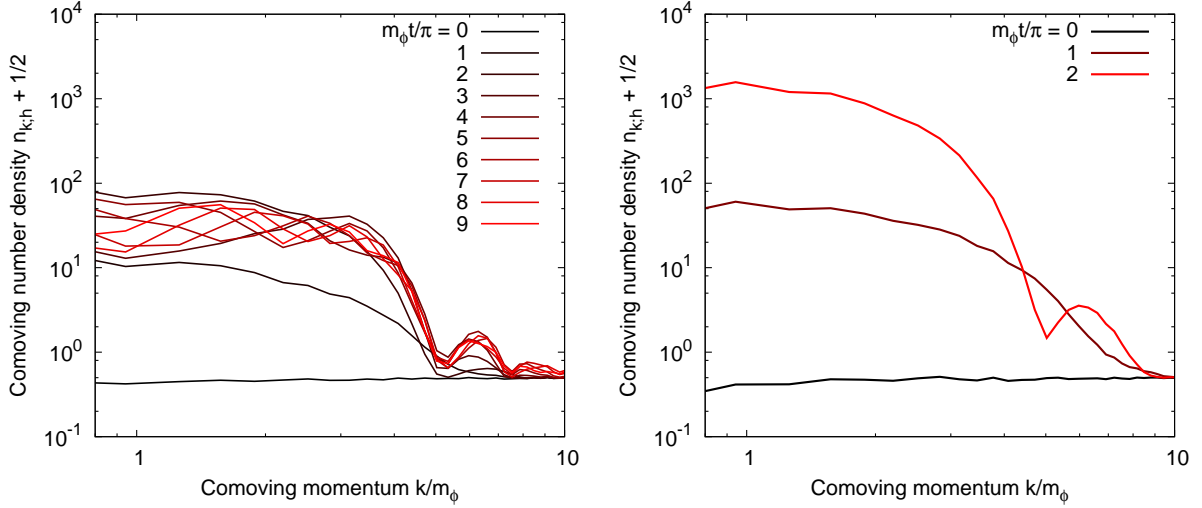


Figure 4: Time evolution of the comoving number density of Higgs. We take the parameters as $N = 128^3$, $dt = 10^{-3}/m_\phi$, $L = 20/m_\phi$, $m_\phi = 1.5 \times 10^{13}$ GeV and $\Phi_{\text{ini}} = \sqrt{2}M_{\text{pl}}$. Left panel: $\xi = 10$. Right panel: $\xi = 20$. We evaluate the number density at the end points of the oscillations. We show the number density only before Higgs rolls down to the true vacuum for the right panel.

We solve the following classical equations of motion in the configuration space:

$$0 = \ddot{\phi} + 3H\dot{\phi} - \frac{1}{a^2}\partial_i^2\phi + 2\frac{\xi}{M_{\text{pl}}^2}\left[\dot{\phi}\dot{h} - \frac{1}{a^2}\partial_i\phi\partial_i h\right]h + \left(1 + \frac{\xi h^2}{M_{\text{pl}}^2}\right)m_\phi^2\phi, \quad (2.45)$$

$$0 = \ddot{h} + 3H\dot{h} - \frac{1}{a^2}\partial_i^2 h + \frac{\xi}{M_{\text{pl}}^2}\left[2m_\phi^2\phi^2 - \dot{\phi}^2 + \frac{1}{a^2}(\partial_i\phi)^2\right]h + \lambda h^3, \quad (2.46)$$

for the scalar fields, and

$$H^2 = \frac{\langle\rho\rangle}{3M_{\text{pl}}^2}, \quad (2.47)$$

for the metric, where the energy density is given by

$$\rho = \frac{1}{2}\left(1 + \frac{\xi h^2}{M_{\text{pl}}^2}\right)\left(\dot{\phi}^2 + \frac{1}{a^2}(\partial_i\phi)^2\right) + \frac{1}{2}\left(1 + 2\frac{\xi h^2}{M_{\text{pl}}^2}\right)m_\phi^2\phi^2 + \frac{1}{2}\left(\dot{h}^2 + \frac{1}{a^2}(\partial_i h)^2\right) + \frac{\lambda}{4}h^4. \quad (2.48)$$

Namely, we solve the equations in the Einstein frame. We only keep up to first-order terms in $\xi h^2/M_{\text{pl}}^2$ and $\xi^2 h^2/M_{\text{pl}}^2$. This treatment is justified because $\xi h^2/M_{\text{pl}}^2, \xi^2 h^2/M_{\text{pl}}^2 \ll 1$ always holds in our numerical calculation. We take the grid number as $N = 128^3$ with a comoving edge size being $L = 20/m_\phi$ for the initial inflaton amplitude $\Phi_{\text{ini}} = \sqrt{2}M_{\text{pl}}$ and $L = 40/m_\phi$ for $\Phi_{\text{ini}} = \sqrt{0.2}M_{\text{pl}}$ ²⁴ and the time step as $dt = 10^{-3}/m_\phi$. We fix the inflaton mass as $m_\phi = 1.5 \times 10^{13}$ GeV. Some details of our numerical calculation are summarized below (the same as those in the quartic coupling case):

- We start to solve the classical equations of motion with $\Phi_{\text{ini}} = \sqrt{2}M_{\text{pl}}$ or $\sqrt{0.2}M_{\text{pl}}$. We set the initial velocity as $\dot{\Phi}_{\text{ini}} = 0$. We introduce gaussian initial fluctuations in the inflaton and Higgs fields which arise from the quantum fluctuations.

²⁴ The typical momentum of our interest is smaller than that in the quartic coupling case. This is why we take the comoving edge size smaller than that in the quartic coupling case here.

- We renormalize masses of inflaton and Higgs originating from the initial quantum fluctuations. See App. B for more details on this procedure.
- We use the redundancy of the equations of motion for the metric as a check of our numerical calculation, and verified that our numerical calculation satisfies the redundancy at least at $\mathcal{O}(10^{-3})$ precision.
- We add a sextic term to the Higgs potential to stabilize it in our calculation. We take the coefficient such that the Higgs field value at the true minimum is $\tilde{\lambda} h_{\min}^2 = 5 \times 10^{-8} M_{\text{pl}}^2$.

In Fig. 3, we show the time evolution of the inflaton vacuum expectation value squared $\langle \phi \rangle^2$ (black), the inflaton dispersion $\langle \phi^2 \rangle - \langle \phi \rangle^2$ (red) and the Higgs dispersion $\langle h^2 \rangle$ (blue), which are multiplied by the scale factor to the third whose initial value is $a_{\text{ini}} = 1$. Again, note that the dispersions are related with the statistical function. We take the Higgs-curvature coupling and the initial inflaton amplitude as follows: $\xi = 10$ and $\Phi_{\text{ini}} = \sqrt{2} M_{\text{pl}}$ for the upper left panel, $\xi = 20$ and $\Phi_{\text{ini}} = \sqrt{2} M_{\text{pl}}$ for the upper right panel, $\xi = 20$ and $\Phi_{\text{ini}} = \sqrt{0.2} M_{\text{pl}}$ for the lower left panel and $\xi = 30$ and $\Phi_{\text{ini}} = \sqrt{0.2} M_{\text{pl}}$ for the lower right panel, respectively.

For the $\Phi_{\text{ini}} = \sqrt{2} M_{\text{pl}}$ cases (the upper panels), the Higgs field remains in the electroweak vacuum for $\xi = 10$, while it rolls down to the true vacuum for $\xi = 20$. Thus, the condition (2.44) is consistent with our numerical calculation within a factor of two.^{♡25} On the contrary to the quartic coupling case, the critical value of the Higgs-curvature coupling depends on Φ_{ini} . Indeed, for the $\Phi_{\text{ini}} = \sqrt{0.2} M_{\text{pl}}$ cases (the lower panels), Higgs remains in the electroweak vacuum for $\xi = 20$, while it rolls down to the true vacuum for $\xi = 30$. Again, it is consistent with our estimation (2.44) once we include the effect of $n_{\text{eff}} \simeq 1.5\text{-}2$.

In Fig. 4, we also plot the time evolution of the comoving number density of Higgs [Eq. (2.14)] for $\Phi_{\text{ini}} = \sqrt{2} M_{\text{pl}}$. The curvature coupling is $\xi = 10$ for the left panel and $\xi = 20$ for the right panel, respectively. We have evaluated the number density at the end points of the oscillations since it is well-defined only at around these points for the curvature coupling case. Higgs is created dominantly within the first few oscillations. This is because the growth rate depends on the inflaton amplitude. The time evolution of the number density for $\Phi_{\text{ini}} = \sqrt{0.2} M_{\text{pl}}$ are quite similar.

3 Higgs-Radiation Coupling

In the previous section, we have neglected the interactions between Higgs and radiation via Yukawa and gauge couplings to illustrate the impacts of Higgs-inflaton coupling. In this section, we investigate whether finite density corrections from the Higgs-radiation coupling could relax the bounds (2.29) and (2.44). In contrast to the vacuum corrections, which destabilize the Higgs potential via fermion loops (*i.e.* top quark), finite density corrections tend to stabilize the Higgs field to its enhanced symmetry point once top quarks and/or electroweak gauge bosons are produced. There are three ways to produce these particles in the course of reheating dynamics:

Instant preheating: For a relatively large Higgs-inflaton coupling, Higgs produced non-perturbatively at $\phi \sim 0$ decays into top quarks within one oscillation at a large field value of inflaton where Higgs becomes heavy [57]. If this decay is prompt, the efficiency of the

^{♡25} The difference between Eq. (2.44) and our numerical calculation may be due to the fact that the inflaton amplitude decreases drastically within the first oscillation for $\Phi_{\text{ini}} = \sqrt{2} M_{\text{pl}}$, while we assume that the amplitude is constant to derive Eq. (2.44). Our main purpose is, however, an order estimation of the critical value of the curvature coupling, and hence Eq. (2.44) is enough.

broad/tachyonic resonance is reduced and the decay products stabilize the Higgs at its enhanced symmetry point.

Annihilation: If the number density of Higgs becomes large owing to the broad/tachyonic resonance, the annihilation of Higgs into top quarks and electroweak gauge bosons becomes significant [58, 59]. This reduces the efficiency of resonance. Also produced top quarks and gauge bosons may stabilize the Higgs at its enhanced symmetry point.

Complete reheating: The Higgs-inflaton/-curvature coupling alone cannot lead to a complete decay of inflaton, and hence an additional interaction of inflaton which completes the reheating is required. Since the radiation is produced before the complete decay of inflaton via this interaction [60–62], the abundant top quarks and electroweak gauge bosons may stabilize the Higgs at its enhanced symmetry point.

We discuss first two effects in this section. To avoid complications, effect of the complete reheating is explained in Sec. 4.3 because it depends on another unknown parameter, *i.e.* reheating temperature.

3.1 Instant preheating

Since Higgs couples with top quarks via the sizable Yukawa coupling, it decays into top quarks at a large field value region of inflaton. The decay might affect the preheating dynamics in two ways: (i) reduce the efficiency of Higgs production, (ii) stabilize the Higgs potential by the screening mass term from decay products. We first give an overview of these effects below.

At the early stage of the preheating, the dynamics depends on the stabilization mechanism. For the quartic stabilization $c^2\phi^2h^2$, the efficiency of the resonance is independent of the coupling c . Hence, the Higgs decay, which is proportional to c , dominates over the Higgs resonant production at the early epoch. Radiation is effectively produced via the Higgs decay at this epoch, and it may stabilize the Higgs potential. It corresponds to the effect (ii). For the curvature stabilization $\xi R h^2$, on the contrary, both the efficiency of the resonance and the decay is proportional to ξ . Thus, the resonant Higgs production always dominates over the Higgs decay, and the effect (ii) is negligible. At the late stage, the Higgs resonant production dominates over the Higgs decay even in the case of the quartic stabilization. Hence, the Higgs decay just reduces the efficiency of the Higgs resonant production for both the quartic/curvature stabilization, which corresponds to the effect (i).

From now we discuss the effects (i) and (ii) in detail. We first consider the effect (i), neglecting the effect (ii). Then we discuss the effect (ii) for the quartic coupling case. We will see that it is relevant only if the Higgs-inflaton coupling is quite large, say $c \gtrsim \mathcal{O}(10^{-1})$.

Slow decay of Higgs [Late stage]

First, let us concentrate on the first effect (i). Thus, we neglect the second effect (ii), assuming that the resonance is not terminated by the back-reaction of decay products. We discuss the quartic stabilization in detail. A similar discussion holds for the curvature stabilization.

We estimate a typical decay rate of Higgs boson by taking an oscillation average, which gives $\bar{\Gamma}_{h \rightarrow t\bar{t}} = (3\alpha_t/2)\bar{m}_{H,h} \sim (3\alpha_t/2\sqrt{2})c\Phi$. Here the bar indicates the oscillation average, $\Gamma_{h \rightarrow t\bar{t}}$ is the decay rate of Higgs into top quarks, $m_{H,h}$ is the effective mass of Higgs, and $\alpha_t \equiv y_t^2/(4\pi) \sim 0.02$ is the top Yukawa coupling at $m_\phi \sim 10^{13}$ GeV. The decay reduces the growth

of Higgs fluctuations as $n_h \propto e^{2\mu m_\phi t - \bar{\Gamma}_{h \rightarrow \bar{t}t}}$. As a result, the decay time given in Eq. (2.27) becomes slightly longer:

$$m_\phi t_{\text{dec}} \sim \frac{1}{2\mu_{\text{qtc}}} \ln \left(\frac{16\pi^{\frac{3}{2}}}{3\tilde{\lambda}} \right) + \frac{\sqrt{3}\alpha_t}{2\mu_{\text{qtc}}} \frac{cM_{\text{pl}}}{m_\phi}. \quad (3.1)$$

By comparing it with t_{end} given in Eq. (2.28), we estimate the impacts of the Higgs decay on the upper bound [Eq. (2.29)] as follows:

$$c \lesssim 10^{-4} \left[\frac{0.1}{\mu_{\text{qtc}}} \right] \left[\frac{m_\phi}{10^{13} \text{ GeV}} \right] \left[1 - 0.1 \left(\frac{\alpha_t}{0.02} \right) \left(\frac{0.1}{\mu_{\text{qtc}}} \right) \right]^{-1}. \quad (3.2)$$

Similarly, in the case of the curvature stabilization, we find

$$\xi \lesssim 10 \times \left[\frac{2}{n_{\text{eff}} \mu_{\text{crv}}} \right]^2 \left[\frac{\sqrt{2} M_{\text{pl}}}{\Phi_{\text{ini}}} \right]^2 \left[1 - 0.04 \left(\frac{\alpha_t}{0.02} \right) \left(\frac{2}{\mu_{\text{crv}}} \right) \right]^{-2}. \quad (3.3)$$

Even if we optimistically estimate the decay rate of Higgs, the effect (i) does not change the upper bound by a large amount, within uncertainties of our order of magnitude estimation. Note here that the decay of Higgs fluctuations into top quarks may be much suppressed in reality. This is because the typical life time of Higgs is prolonged for Higgs fluctuations are relativistic, and because the top quarks acquire a finite density mass correction from the Higgs fluctuations, which could suppress the Higgs decay into two top quasi-particles kinematically. Since the purpose of this subsection is to confirm that our estimation is not affected even if we take into account the effect (i), we do not further investigate this effect.

Instant decay of Higgs [Early stage]

The next step is to include the second effect (ii). As we saw at the beginning of this subsection, the Higgs decay dominates over the Higgs resonant production at the early epoch of the preheating stage for the quartic coupling case. In fact, for a sizable coupling c , the resonance can be killed by the back-reaction of decay products of Higgs.

If the quartic coupling c satisfies $\bar{\Gamma}_{h \rightarrow \bar{t}t} \gg m_\phi / \pi \leftrightarrow \pi \alpha_t c \Phi \gg m_\phi$, Higgs produced at $\phi \sim 0$ decays completely before the inflaton moves back to its potential origin $\phi \sim 0$. While this condition holds, the inflaton decays with the following rate [63, 64]:²⁶

$$\Gamma_{\text{inst}} \sim \frac{c^2}{4\pi^4 [3\alpha_t/2]^{\frac{1}{2}}} m_\phi \quad \text{for } \pi \alpha_t c \Phi(t) \gg m_\phi. \quad (3.4)$$

Contrary to the previous case, one can show that the Higgs becomes non-relativistic at its decay. Also, the effective mass of top quarks from the Higgs fluctuations can be safely neglected because the effective mass of Higgs from the inflaton field at its decay is sufficiently large in this case. Assuming that the conditions, $\pi \alpha_t c \Phi(t) \gg m_\phi$ and $p_*^2 > \delta m_{\text{th},h}^2$, hold at $\Gamma_{\text{inst}} \sim H$, one can estimate the ‘‘reheating temperature’’ as follows:

$$T_{\text{inst}} \sim \left(\frac{90}{\pi^2 g_*} \right)^{\frac{1}{4}} \sqrt{\Gamma_{\text{inst}} M_{\text{pl}}} \simeq 4 \times 10^{13} \text{ GeV} \left[\frac{c}{0.1} \right] \left[\frac{0.02}{\alpha_t} \right]^{\frac{1}{4}} \left[\frac{100}{g_*} \right]^{\frac{1}{4}} \left[\frac{m_\phi}{1.5 \times 10^{13} \text{ GeV}} \right]^{\frac{1}{2}}, \quad (3.5)$$

²⁶ Here note that once the condition, $\pi \alpha_t c \Phi(t) \gg m_\phi$, is violated owing to the reduction of inflaton amplitude, e.g. by the cosmic expansion, the effective decay rate of inflaton becomes $\sim \Gamma_{\text{inst}} \times [(\sqrt{3}\pi/2)(\alpha_t c \Phi/m_\phi)^{3/2}]$, which decreases faster than the Hubble parameter.

where g_* is the relativistic degrees of freedom produced via this process. The amplitude of inflaton at that time is estimated as $\Phi_{\text{inst}} \sim 10^{15} \text{ GeV} [0.02/\alpha_t]^{1/2} [c/0.1]^2$. Both conditions, $\pi\alpha_t c\Phi \gg m_\phi$ and $p_*^2 > \delta m_{\text{th};h}^2$, are satisfied for $c \gtrsim 0.1$ at that time. Moreover, for a large enough coupling $c \gg 0.1$, the resonance may be terminated by the back-reaction, and the inflaton itself might participate in thermal plasma. If this is really the case, the coherence of inflaton is lost, and the resonance becomes inefficient.

In this paper, we do not concretely estimate the coupling c above which the inflaton participates in the thermal plasma, for the following reasons. First of all, the quartic interaction yields the Coleman-Weinberg potential [65]:

$$V_{\text{CW}} = \frac{c^4}{64\pi^2} \phi^4 \ln \frac{c^2 \phi^2}{m_\phi^2}. \quad (3.6)$$

If we stick to the quadratic potential (2.2), the coupling c is bounded from above $c \lesssim 10^{-3}$ [66]. In this case, the instant preheating is not efficient. In addition, for $c \gtrsim 0.1$,^{♡27} a flattening mechanism of the inflaton potential may be required; examples are the non-minimal coupling [37] or the modified kinetic terms [38, 41, 42]. In these cases, the inflaton potential is more complicated, and in particular, it is dominated by the ϕ^4 term below a threshold field value of ϕ that depends on model parameters. Since the energy density of inflaton behaves as radiation below this scale, the resonance does not take place once $p_*^2 \sim \delta m_{\text{th};h}^2$ is saturated. Eventually, the whole system, including inflaton, might be thermalized through thermal dissipations [69]. We postpone this issue to avoid model dependent discussions.

3.2 Annihilation

In the broad/tachyonic resonance, the number density of Higgs grows exponentially. If the number density is large enough, Higgs can annihilate into top quarks and electroweak gauge bosons. In particular, Higgs may rapidly excite the gauge bosons to exponentially large number densities [70]. If the number densities of these particles become comparable to that of Higgs before it rolls down to the true vacuum, they might stabilize Higgs since the gauge coupling is larger than the Higgs quartic coupling.

In order to see whether the annihilation process can stabilize the electroweak vacuum during the preheating stage, we consider the following simplified Lagrangian:

$$\mathcal{L} = \mathcal{L}_{\text{inf}}(\phi) + \mathcal{L}_{\text{Higgs}}(h) + \mathcal{L}_\chi(\chi) + \mathcal{L}_{\text{int}}(\phi, h) + \mathcal{L}_{\text{ann}}(h, \chi), \quad (3.7)$$

where $\mathcal{L}_{\text{inf}}(\phi)$, $\mathcal{L}_{\text{Higgs}}(h)$ and $\mathcal{L}_{\text{int}}(\phi, h)$ are the same as those given in Eqs. (2.2), (2.3) and (2.5), and

$$\mathcal{L}_\chi(\chi) = \frac{1}{2} \partial_\mu \chi \partial^\mu \chi - \frac{1}{4} g_{\chi\chi}^2 \chi^4, \quad (3.8)$$

$$\mathcal{L}_{\text{ann}}(h, \chi) = -\frac{1}{2} g_{h\chi}^2 h^2 \chi^2. \quad (3.9)$$

Here the light field χ schematically represents the SM gauge bosons, and we model the gauge interactions as the quartic interactions.

^{♡27} The inflaton-Higgs coupling can affect the RGE running of the Higgs quartic coupling at the energy scale higher than m_ϕ . It may lead to the absolute stability of the Higgs potential for $c \gtrsim 1$, which is out of our interest. Note that the mechanism of Refs. [67, 68] to make the Higgs potential stable does not work in the present model, since the Z_2 symmetry $\phi \rightarrow -\phi$ is not broken at the present vacuum.

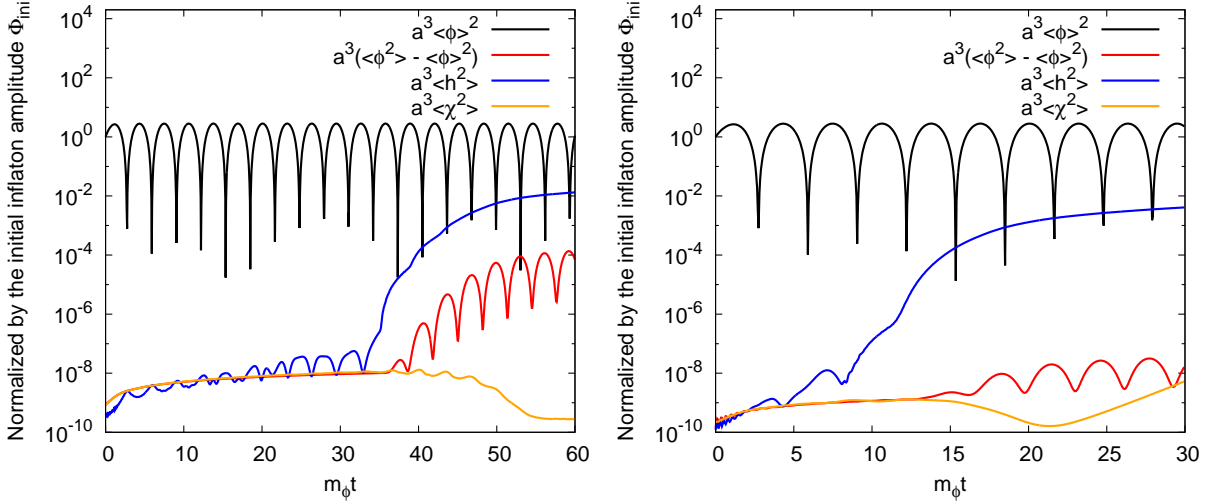


Figure 5: Numerical calculation of the time evolution of the inflaton expectation value (black), the inflaton dispersion (red), the Higgs dispersion (blue) and the χ dispersion (orange). We plot the quartic coupling case for the left panel and the curvature coupling case for the right panel, respectively. We take the parameters as $N = 128^3$, $dt = 10^{-3}/m_\phi$, $m_\phi = 1.5 \times 10^{13}$ GeV, $\Phi_{\text{ini}} = \sqrt{2} M_{\text{pl}}$ and $g_{h\chi} = g_{\chi\chi} = 0.5$. Left panel: $c = 2 \times 10^{-4}$ and $L = 10/m_\phi$. Right panel: $\xi = 20$ and $L = 20/m_\phi$. The annihilation processes cannot save the electroweak vacuum.

We have solved the classical equations of motion derived from the Lagrangian (3.7) numerically. We take $N = 128^3$, $dt = 10^{-3}/m_\phi$, $m_\phi = 1.5 \times 10^{13}$ GeV, $\Phi_{\text{ini}} = \sqrt{2} M_{\text{pl}}$, $a_{\text{ini}} = 1$, $\dot{\Phi}_{\text{ini}} = 0$ and $g_{h\chi} = g_{\chi\chi} = 0.5$. We summarize some details of our numerical calculation below:

- We introduce gaussian initial fluctuations in the inflaton, Higgs and χ fields which arise from the quantum fluctuations.
- We renormalize masses of inflaton, Higgs and χ originating from the initial quantum fluctuations. See App. B for more details on this procedure.
- We have used the redundancy of the equations of motion for the metric as a check of our numerical calculation. We have verified that our numerical calculation satisfies the redundancy at least at $\mathcal{O}(10^{-3})$ precision.
- We add a sextic term to the Higgs potential to stabilize it in our calculation. We take the coefficient such that the Higgs field value at the true minimum is $\tilde{\lambda} h_{\text{min}}^2 = 5 \times 10^{-8} M_{\text{pl}}^2$.
- In the case of the curvature coupling, we solve the equations of motion in the Einstein frame. We have taken only up to first-order terms in $\xi h^2/M_{\text{pl}}^2$ and $\xi^2 h^2/M_{\text{pl}}^2$. This is because $\xi h^2/M_{\text{pl}}^2, \xi^2 h^2/M_{\text{pl}}^2 \ll 1$ always holds in our numerical calculation.

In Fig. 5, we show the time evolution of the inflaton vacuum expectation value squared $\langle \phi \rangle^2$ (black), the inflaton dispersion $\langle \phi^2 \rangle - \langle \phi \rangle^2$ (red), the Higgs dispersion $\langle h^2 \rangle$ (blue) and the χ dispersion $\langle \chi^2 \rangle$ (orange). They are multiplied by the scale factor to the third. The left panel is the result of the quartic coupling case with $c = 2 \times 10^{-4}$ and $L = 10/m_\phi$, and the right panel is that of the curvature coupling case with $\xi = 20$ and $L = 20/m_\phi$. As we can see from Fig. 5, Higgs rolls down to the true vacuum well before χ is sufficiently produced. In fact, the dynamics of Higgs is almost the same as those in Figs. 1 and 3. Thus, the annihilation

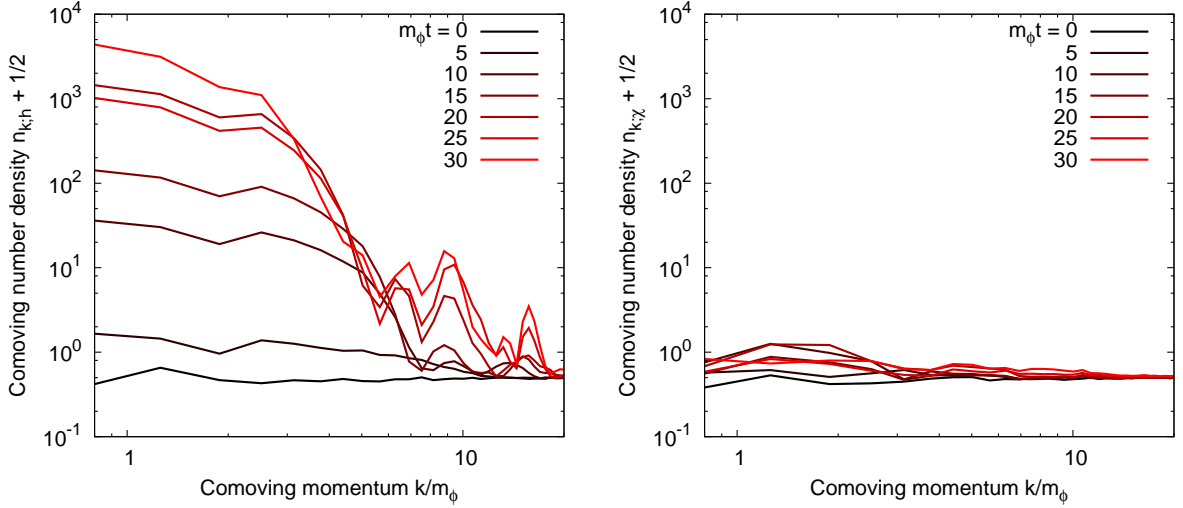


Figure 6: We plot the spectra of Higgs and χ for the quartic coupling case. Left panel: the spectrum of Higgs. Right panel: the spectrum of χ . Higgs is resonantly produced, while χ is not efficiently produced.

process cannot stabilize the electroweak vacuum in our simplified setup. The results do not change even if we take the couplings of χ larger, say $g_{h\chi} = g_{\chi\chi} = 1$.

Now let us take a closer look at Fig. 5. For the curvature coupling case, Higgs rolls down to the true vacuum at the first few oscillation of inflaton, regardless of the existence of the annihilation channel. It seems that this is because the time scale of the electroweak vacuum decay is too short for the annihilation to be effective. We believe that the same argument also holds for the realistic model where Higgs couples to the electroweak gauge bosons, since the annihilation rate is not much different from that of our simplified model.

For the quartic coupling case, Higgs remains in the electroweak vacuum for the first $\mathcal{O}(1-10)$ times of oscillation of inflaton. Even in such a case, however, χ is not efficiently produced via the annihilation process. To see this, we plot the spectrum of Higgs and χ for the quartic coupling case in Fig. 6. We can see that Higgs is resonantly produced, while χ is not efficiently produced. This behavior may be understood as follows. If Higgs is resonantly produced, it induces an effective mass to χ as a finite density correction:

$$m_{\text{eff};\chi}^2(t) = g_{h\chi}^2 \int_{\mathbf{k}/a(t)} \frac{1}{2} G_{F;h}(t, t; \mathbf{k}) \simeq g_{h\chi}^2 \frac{n_h(t)}{\omega_{k*;h}(t)}. \quad (3.10)$$

The phase space of the produced χ is kinematically restricted by the effective mass $m_{\text{eff};\chi}^2$, and hence it may suppress the annihilation rate.^{♡28} Provided that this description is correct, the dynamics should be similar for the realistic case where Higgs couples to the gauge bosons. The resonant production of Higgs induces effective masses to the gauge bosons, and hence we expect that the annihilation of Higgs into the gauge bosons is suppressed in the same way as our simplified model. Thus, we believe that the annihilation process cannot stabilize the electroweak vacuum during the preheating stage in the realistic case either. More rigorous analysis requires classical lattice simulations including SM gauge bosons [71, 72] and fermions, which is beyond the scope of this paper.

Note that, even if we properly take into account the degrees of freedom of the gauge boson and Higgs, the situation is not expected to change. The reason is the following. In

^{♡28} As an extreme case, the annihilation process is kinematically forbidden if $m_{\text{eff};\chi} \gg p_*$.

order for the gauge boson to stabilize Higgs, its dispersion must satisfy

$$g^2 \sum \langle A^2 \rangle \sim |\lambda| \sum \langle h^2 \rangle, \quad (3.11)$$

where the sums are for the six degrees of freedom for the gauge boson A and the four degree of freedom for Higgs h , respectively. Expecting that $\langle A^2 \rangle \simeq \langle \chi^2 \rangle$, we can see from Figs. 5 and 6 that the produced amount of the gauge boson is far below Eq. (3.11).

It is noticeable that it depends on the numerical value of the Higgs quartic coupling whether the annihilation can stabilize the electroweak vacuum or not. In the present case with the center value of top quark mass, the Higgs quartic coupling is rather large, $\tilde{\lambda} \sim 0.01$, and hence the annihilation cannot catch up the vacuum decay. However, it can stabilize the electroweak vacuum if $\tilde{\lambda}$ is small enough. It may be worth studying further on this respect.

4 After Preheating

So far we have focused on the stability of Higgs during the preheating stage. We have obtained the robust bound on the Higgs-inflaton coupling above which Higgs rolls down to its true vacuum. In this section, we consider the dynamics of Higgs after the preheating stage in the case where the electroweak vacuum survives the preheating stage. We study whether or not the dynamics after the preheating forces the electroweak vacuum to decay. For notational simplicity, we denote the effective mass of Higgs induced by the Higgs-inflaton/-curvature coupling as $m_{H;h}^2$. It is given by $m_{H;h}^2 = c^2 \Phi^2(t)/2$ for the Higgs-inflaton coupling and $m_{H;h}^2 = \xi m_\phi^2 \Phi^2(t)/2M_{\text{pl}}^2$ for the Higgs-curvature coupling [See Eqs. (2.16) and (2.36)].

First we summarize basic properties of Higgs fluctuations just after the preheating stage. At $t = t_{\text{end}}$, $m_{H;h}$ is comparable to the inflaton mass, $m_{H;h}(t_{\text{end}}) \simeq m_\phi$. The physical momentum scale of Higgs is estimated as $p_*(t_{\text{end}}) \simeq m_\phi \simeq m_{H;h}(t_{\text{end}})$. Since we assume that the electroweak vacuum survives the preheating stage, the tachyonic effective mass term of Higgs induced by its self interaction satisfies $|\delta m_{\text{self};h}(t_{\text{end}})| < p_*(t_{\text{end}}) \simeq m_{H;h}(t_{\text{end}})$. Therefore, all wave length modes are stable against the tachyonic mass term just after the preheating.^{♡29} As one can guess from Figs. 2 and 4, the comoving number density in a momentum space at $t = t_{\text{end}}$ may be approximated as

$$n_{k;h}(t_{\text{end}}) = \begin{cases} f & \text{for } H \ll k/a_{\text{end}} \lesssim m_\phi \\ k^{-n} & \text{for } m_\phi \lesssim k/a_{\text{end}} \end{cases}, \quad (4.1)$$

with $n \geq 4$. The stability condition, $m_\phi^2 > |\delta m_{\text{self};h}(t_{\text{end}})|$, puts a rough upper bound $f \lesssim 10^3 \times (10^{-2}/\tilde{\lambda})$. A characteristic coupling of this system is roughly, $\alpha, \alpha_t \sim 0.02\text{--}0.1$, where α is the fine structure constant of the SM gauge group. Let us parametrize the typical value of Higgs distribution as $f = \alpha^{-m}$. The Higgs distribution mostly lies in the “*over-occupied*” regime, $0 < m < 1$; or “*extremely over-occupied*” regime, $1 < m$ [73], at the boundary of the inequalities (2.29) and (2.44).

A complete analysis of this system after the preheating stage is beyond the scope of paper. Instead, we discuss its possible processes, and point out important ingredients which could change the dynamics qualitatively.

^{♡29} See the $q < 1$ and $0 < A_k < 1$ region of the stability/instability chart of the Mathieu equation in Ref. [31].

4.1 Cosmic expansion

First, let us discuss the effect of cosmic expansion. As an illustration, let us consider only the effective masses induced by the Higgs-inflaton coupling and the Higgs self interaction. The mass term $m_{H;h}^2$ decreases as $m_{H;h}^2 \propto a^{-3}$ since the inflaton harmonically oscillates with time. On the other hand, the effective mass of Higgs induced by the its self coupling follows $\delta m_{\text{self};h}^2 \propto a^{-2}$. This is because the modes with the momentum $p \sim p_*$ or $p_*^{(\text{tac})}$ dominate the Higgs dispersion, and hence we can treat them as relativistic particles.

Right after the end of the preheating, the mass term $m_{H;h}^2$ stabilizes the electroweak vacuum against the tachyonic mass term $\delta m_{\text{self};h}^2$ generated by the Higgs self interaction. However, since $m_{H;h}^2$ decreases faster than $\delta m_{\text{self};h}^2$, the long wave length mode of Higgs may be destabilized eventually. We now estimate the time scale t_{eq} when the inflaton induced mass becomes comparable to the tachyonic mass. For the quartic stabilization, we get

$$m_\phi t_{\text{eq}} \sim 6 \times 10^3 \left[\frac{c}{10^{-4}} \right]^{\frac{7}{4}} \exp \left[-7.8 \times \left(\frac{c}{10^{-4}} - 1 \right) \right]. \quad (4.2)$$

Here we focus on the coupling c dependence, and take $\mu_{\text{qtc}} = 0.1$ and $m_\phi = 1.5 \times 10^{13}$ GeV. For the curvature stabilization, the time scale is estimated as

$$m_\phi t_{\text{eq}} \sim 2 \times 10^3 \left[\frac{\xi}{2} \right]^{\frac{3}{4}} \left[\frac{\Phi_{\text{ini}}}{\sqrt{2} M_{\text{pl}}} \right]^{\frac{1}{2}} \exp \left[-6 \times \left(\sqrt{\frac{\xi}{2}} \frac{n_{\text{eff}} \mu_{\text{crv}}}{2} \frac{\Phi_{\text{ini}}}{\sqrt{2} M_{\text{pl}}} - 1 \right) \right]. \quad (4.3)$$

Here we take $m_\phi = 1.5 \times 10^{13}$ GeV.

If the Higgs self coupling λ is still negative at $t = t_{\text{eq}}$, Higgs eventually rolls down to the true vacuum. For the electroweak vacuum not to decay after the preheating, $\langle h^2 \rangle$ should be smaller than h_{max}^2 at $t = t_{\text{eq}}$. Thus, we derive the upper bounds on the couplings as

$$c \lesssim 3 \times 10^{-5} \left[\frac{0.1}{\mu_{\text{qtc}}} \right] \left[\frac{m_\phi}{1.5 \times 10^{13} \text{ GeV}} \right] \left[1 + 0.4 \ln \left(\frac{h_{\text{max}}/10^{10} \text{ GeV}}{m_\phi/1.5 \times 10^{13} \text{ GeV}} \right) \right], \quad (4.4)$$

for the quartic stabilization, and

$$\xi \lesssim 7 \times 10^{-1} \left[\frac{2}{n_{\text{eff}} \mu_{\text{crv}}} \right]^2 \left[\frac{\sqrt{2} M_{\text{pl}}}{\Phi_{\text{ini}}} \right]^2 \left[1 + 0.3 \ln \left(\frac{h_{\text{max}}/10^{10} \text{ GeV}}{m_\phi/1.5 \times 10^{13} \text{ GeV}} \right) \right]^2, \quad (4.5)$$

for the curvature stabilization.^{♡30} Interestingly, almost all the parameters required to stabilize the electroweak vacuum during inflation results in the catastrophe, unless there exist other contributions to the Higgs effective mass term. Thus, the inclusion of Higgs-radiation coupling is crucial.

4.2 Turbulence and thermalization

Next, let us discuss how the Higgs-radiation coupling could change these bounds qualitatively. In this section, we neglect radiation generated in the process of complete reheating, assuming that the reheating temperature is low enough. See also the discussion in the next subsection.

^{♡30} It should be regarded as an illustration since the condition for the resonance to occur is only marginally satisfied at these values.

Higgs couples with electroweak gauge bosons and top quark via gauge and top Yukawa couplings. The initial Higgs distribution illustrated in Eq. (4.1) is eventually thermalized while producing SM particles, and its thermalization time scale is characterized by these couplings. Once it is thermalized, the lifetime of our vacuum can be estimated by means of the thermal bounce [5, 8]. In particular, it was shown in Ref. [74] that the lifetime of the electroweak vacuum is long enough if we adopt the central value of the top quark mass. Therefore, we expect that the electroweak vacuum is stable if thermalization time scale is much shorter than t_{eq} .

Now we roughly estimate the thermalization time scale. As shown in Refs. [75–77], an initially over-occupied system, like Eq. (4.1), enters the turbulent regime at first, cascades self-similarly, and eventually attains thermal distribution. In addition, the IR cascade may develop the long wave length mode as pointed out in Ref. [77, 78], and might boost the vacuum decay. Here, however, as an illustration, we simply compare the typical time scale of elastic scatterings with the Hubble parameter. In fact, for a mildly over-occupied system, its thermalization may be dominated by the elastic scatterings [73, 76]. This is the case of $c \lesssim 10^{-4}$ for the quartic coupling and $\xi \lesssim 1$ for the curvature coupling, though it strongly depends on which interaction dominates the thermalization. The thermalization time of elastic scatterings may be evaluated as $\alpha^2 T^{(\text{w.b.})}(t_{\text{th}}) \sim H(t_{\text{th}})$ with $T^{(\text{w.b.})}(t)$ being an would-be temperature when the system at that time t would be thermalized. We find that the thermalization time scale, t_{th} , is much longer than or at most comparable to t_{eq} for the parameter region of our interest. Further studies on this case will be presented elsewhere.

4.3 Complete reheating

Finally, we study the effective mass of Higgs from radiation generated during the process of the complete reheating. Since the Higgs-inflaton/-curvature coupling alone cannot lead to a complete decay of inflaton, an additional interaction of inflaton which completes the reheating is required. We discuss how it affects the dynamics of Higgs both during and after the preheating in the following.

To discuss the complete reheating process in detail [61, 62], we have to specify the interaction between inflaton and radiation, which strongly depends on inflationary models. In the following discussion, we focus on the case where inflaton reheats the Universe via Planck-suppressed operators; the decay rate of inflaton is given by

$$\Gamma_\phi = \frac{\tilde{\Gamma}_\phi m_\phi^3}{M_{\text{pl}}^2}. \quad (4.6)$$

Here $\tilde{\Gamma}_\phi$ is a constant that is smaller than unity $\tilde{\Gamma}_\phi \ll 1$. For a dimension-five Planck-suppressed decay of inflaton, we may expect $\tilde{\Gamma}_\phi \sim \mathcal{O}(0.1)$. At the end of the next sub-section, we briefly comment on the case with slightly larger couplings between inflaton and radiation.

The “thermal mass” contribution to the Higgs effective potential may be parametrized as

$$\frac{1}{2} \delta m_{\text{th},h}^2 h^2 \theta(h_{\text{th}} - h), \quad (4.7)$$

where θ is the Heaviside step function, $\delta m_{\text{th},h}$ is the “thermal mass” from radiation generated during the course of the complete reheating, and h_{th} is a typical threshold field value above which the electroweak gauge bosons and top quark may not be produced efficiently owing to its large effective mass proportional to the field value of Higgs. Both $\delta m_{\text{th},h}$ and

h_{th} depend on time. See Appendix C for details, and the concrete forms of $\delta m_{\text{th};h}$ and h_{th} for each regime, given in Eqs. (C.1) and (C.2). We expect that the electroweak vacuum is stabilized if both $\delta m_{\text{th};h}^2(t_{\text{eq}}) > |\delta m_{\text{self};h}^2(t_{\text{eq}})|$ and $h_{\text{th}}(t_{\text{eq}}) > \sqrt{\langle h^2(t_{\text{eq}}) \rangle}$ are fulfilled.^{♡31}

During preheating

Here we discuss whether or not the dynamics of the complete reheating would change the upper bound given in Eqs. (2.29) and (2.44).

First of all, let us estimate a relevant time scale in the following discussion. For the quartic stabilization, the longest time scale is governed by Eq. (2.5), which characterizes the end of resonant amplification by the cosmic expansion:

$$m_\phi t_{\text{end}} \simeq 40 \times \left(\frac{c}{10^{-4}} \right) \left(\frac{10^{13} \text{ GeV}}{m_\phi} \right). \quad (4.8)$$

For the curvature stabilization, the dynamics is almost determined by the first few oscillations. Hence, we have to deal with the time scale of $\mathcal{O}(10^{0-2})$ times oscillations of inflaton. Since this time scale is rather short, we cannot rely on the instantaneous thermalization approximation, frequently assumed in literature [24, 60]. To see this, it is instructive to roughly estimate the two-to-two scattering rate because, at least, this interaction should be faster than the cosmic expansion to attain thermal equilibrium. A naive estimation may give the rate of $(\alpha^2/m_s^2) \times n_{\text{rad}} \sim \alpha m_\phi$, where α is the fine structure constant of SM gauge group and the screening mass is given by $m_s^2 \sim \alpha n_{\text{rad}}/m_\phi$. One can see that even the two-to-two scattering does not take place for $m_\phi t \lesssim \alpha^{-1} \sim \mathcal{O}(10)$, which is comparable to the time scale of our interest. The above estimation is too naive, so it should be understood as an illustration. See Appendix C for details.

Let us estimate the effects of radiation produced during the process of complete reheating. Radiation induces the effective potential $\sim \delta m_{\text{th};h}^2 h^2 \theta(h_{\text{th}} - h)$ with $\delta m_{\text{th};h}^2$ and h_{th} depending on time t [See Eqs. (C.1) and (C.2)]. This effective mass is always smaller than the inflaton mass, and thus the condition for the efficient Higgs production given in Eq. (2.20) [Eq. (2.41)] holds: $p_* > m_\phi \gg \delta m_{\text{th};h}$. Also, the condition given in Eq. (2.26) [Eq. (2.43)] holds for $p_* > m_\phi$ because of $|\delta m_{\text{self};h}| > p_* > m_\phi \gtrsim \tilde{\lambda}^{1/2} h_{\text{th}}$. Therefore, in the case of Planck-suppressed decay of inflaton, we expect that the process of complete reheating is not likely to change the upper bound given in Eqs. (2.29) and (2.44). However, note that we have taken a sufficiently small $\tilde{\Gamma}_\phi$ so that resonant particle production of SM particles other than Higgs does not occur. An enhanced $\tilde{\Gamma}_\phi$ might affect the obtained bound. See also discussion in Sec. 5.

After preheating

The dynamics of Higgs after the preheating strongly depends on the reheating dynamics. This is because radiation produced via the complete reheating generates additional Higgs effective mass term, which follows $\delta m_{\text{th};h} \propto a^{-3/8}$ before the complete decay of inflaton. Since it decreases much slower than the tachyonic mass term, this term eventually takes over the dominant contribution of the effective mass.

First, let us discuss a case with $T_{\text{RH}} \simeq 10^{10}$ GeV, which is a typical example of dim. 5 Planck-suppressed decay. For the quartic stabilization with $c \simeq 10^{-4}$, a typical time scale given in

^{♡31} This requirement is somewhat conservative, for the ‘‘thermal mass’’ from hard primaries [Eq. (C.1)] may reduce the Higgs dispersion at the early stage of preheating in the case of $|\delta m_{\text{self};h}| < p_*$.

Eq. (4.2) resides in $m_\phi t_{\text{eq}} \sim 6 \times 10^3 \in [\tilde{t}_{\text{max}}, \tilde{t}_{\text{RH}}]$ for $T_{\text{RH}} \simeq 10^{10}$ GeV [See Eq. (C.2) and definitions below it]. The thermal mass of Higgs at that time is given by

$$\delta m_{\text{th};h}(t_{\text{eq}}) \sim 10^{12} \text{ GeV} \left[\frac{\alpha}{0.1} \right]^{\frac{1}{2}} \left[\frac{\tilde{\Gamma}_\phi}{0.2} \right]^{\frac{1}{4}} \left[\frac{6 \times 10^3}{m_\phi t_{\text{eq}}} \right]^{\frac{1}{4}}, \quad (4.9)$$

with $k_{\text{max}} \sim 10^{12}$ GeV. The effective mass term of Higgs induced from its self interaction at that time is

$$|\delta m_{\text{self};h}(t_{\text{eq}})| \sim 7 \times 10^{10} \text{ GeV} \left[\frac{10^{-4}}{c} \right]^{\frac{3}{4}} \exp \left[7.8 \times \left(\frac{c}{10^{-4}} - 1 \right) \right]. \quad (4.10)$$

For a smaller coupling of c , the equality time, t_{eq} , becomes longer, and it is more likely to be stabilized by the thermal contribution, for the thermal mass decreases slower than the effective mass of Higgs generated from its self interaction. Therefore, we expect that the reheating temperature of $T_{\text{RH}} \simeq 10^{10}$ GeV may save the electroweak vacuum in the case with a quartic coupling of $c \lesssim 10^{-4}$, because the conditions, $\delta m_{\text{th};h} > |\delta m_{\text{self};h}|$ and $h_{\text{th}} = k_{\text{max}}/g > |\delta m_{\text{self};h}|/\tilde{\lambda}^{1/2}$, are satisfied. Also, for the curvature stabilization with $\xi \simeq 2$, the typical time scale shown in Eq. (4.3) resides in $m_\phi t_{\text{eq}} \sim 1.6 \times 10^3 \in [\tilde{t}_{\text{el}}, \tilde{t}_{\text{soft}}]$ for $T_{\text{RH}} \simeq 10^{10}$ GeV [See Eq. (C.2) and definitions below it]. The ‘‘thermal mass’’ of Higgs may be given by

$$\delta m_{\text{th};h}(t_{\text{eq}}) \sim 10^{12} \text{ GeV} \left[\frac{\alpha}{0.1} \right]^{\frac{3}{4}} \left[\frac{\tilde{\Gamma}_\phi}{0.2} \right]^{\frac{3}{8}} \left[\frac{1.6 \times 10^3}{m_\phi t_{\text{eq}}} \right]^{\frac{1}{4}}, \quad (4.11)$$

with $k_{\text{max}} \sim 6 \times 10^{11}$ GeV. The effective mass term of Higgs induced from its self interaction is estimated as

$$|\delta m_{\text{self};h}(t_{\text{eq}})| \sim 2 \times 10^{10} \text{ GeV} \left[\frac{\xi}{2} \right]^{-\frac{1}{4}} \left[\frac{\sqrt{2} M_{\text{pl}}}{\Phi_{\text{ini}}} \right]^{\frac{1}{2}} \exp \left[6 \times \left(\sqrt{\frac{\xi}{2}} \frac{\Phi_{\text{ini}}}{\sqrt{2} M_{\text{pl}}} \frac{n_{\text{eff}} \mu}{2} - 1 \right) \right]. \quad (4.12)$$

Hence, we expect that the reheating temperature of $T_{\text{RH}} \simeq 10^{10}$ GeV may save the electroweak vacuum in the case with a curvature coupling of $\xi \lesssim 2$. Note, however, that we have assumed $\xi \gg 1$ in our estimation, and hence the numerics, $\xi \simeq 2$, should be understood as an illustration.

Next, let us estimate the lower bound of the reheating temperature below which the reheating dynamics cannot save the electroweak vacuum, utilizing the results given in [61, 62]. In order to estimate the lower bound conservatively, we demand that the ‘‘thermal mass’’ term, $\delta m_{\text{th};h}^2$, is always much smaller than the dispersion of Higgs, $\langle h^2 \rangle$, throughout the thermal history up to the equality time t_{eq} . Moreover, strictly speaking, not only the thermal potential but the thermal dissipation might relax the Higgs to its enhanced symmetry point. A complete analysis is beyond the scope of this paper. Instead, we simply require that the thermal interactions are slow enough $\alpha^2 T t_{\text{eq}} \ll 1$, which is essentially the same as $m_\phi t_{\text{eq}} \ll \tilde{t}_{\text{soft}}$. Imposing these requirements, for both the quartic/curvature stabilization, we obtain a rather conservative bound on the reheating temperature below which the reheating dynamics cannot save the electroweak vacuum: $T_{\text{RH}} \lesssim \mathcal{O}(10^5)$ GeV. Anyway, we need further investigations to derive more precise lower bound on the reheating temperature.

5 Conclusions and Discussion

The current experimental data of the Higgs and top quark masses indicates that the electroweak vacuum is metastable if there is no new physics other than the SM. From the view-

point of inflationary cosmology, one interesting consequence is that high-scale inflation requires some stabilization mechanism of Higgs during inflation. A possible candidate of such a mechanism is the Higgs-inflaton/-curvature coupling. In fact, it induces an effective mass and stabilizes Higgs during inflation. After inflation, however, it causes an exponential enhancement of Higgs fluctuations due to the broad/tachyonic resonance, and hence the electroweak vacuum may eventually decay into the true one during the preheating stage.

In this paper, we have focused on the preheating dynamics of Higgs induced by the Higgs-inflaton/-curvature coupling. We have clarified in what parameter space our electroweak vacuum decays into the true one via the broad/tachyonic resonance. We have derived the criterion when Higgs rolls down to the true vacuum, and confirmed it by performing the 3 + 1-dimensional classical lattice simulations. To be concrete, the electroweak vacuum survives the preheating stage only if the couplings satisfy the following inequalities:

$$c \lesssim 10^{-4} \left[\frac{0.1}{\mu_{\text{qtc}}} \right] \left[\frac{m_\phi}{10^{13} \text{ GeV}} \right],$$

for the quartic coupling case, and

$$\xi \lesssim 10 \left[\frac{2}{n_{\text{eff}} \mu_{\text{crv}}} \right]^2 \left[\frac{\sqrt{2} M_{\text{pl}}}{\Phi_{\text{ini}}} \right]^2,$$

for the curvature coupling case, as long as the broad/tachyonic resonance is effective at the onset of the inflaton oscillation. See Eqs. (2.29) and (2.44). These conditions claim that the Hubble expansion should kill the resonance before the Higgs self coupling becomes relevant. In order to suppress the fluctuation of Higgs during inflation, the couplings c and ξ should satisfy $c \gtrsim \mathcal{O}(H_{\text{inf}}/\Phi_{\text{ini}})$ and $\xi \gtrsim \mathcal{O}(0.1)$ [7, 24]. Thus, our results indicate that the Higgs-inflaton/-curvature coupling should be rather small to stabilize Higgs during both the inflation and the preheating stages. We have also seen that the Higgs-radiation coupling does not change the situation as long as the inflaton *perturbatively* reheats the Universe, *i.e.* no resonant particle production occurs except for Higgs. This is the main conclusion of this paper.

Here we give some remarks. First of all, we comment on the dynamics of Higgs after the preheating, in the case where the electroweak vacuum survives during the preheating stage. As explained in Sec. 4.1, if one neglects the Higgs-radiation coupling, the cosmic expansion leads to the decay of our electroweak vacuum for almost all the parameters of our interest [See Eqs. (4.4) and (4.5)]. Thus, including the Higgs-radiation coupling is important to discuss the fate of electroweak vacuum after the preheating. Such an over-occupied system, as illustrated in Eq. (4.1), may exhibit turbulence and cascade towards not only UV but IR, which might have implications on thermalization after the preheating. As a first step, we have simply compared the elastic scattering rate with the Hubble parameter and have seen that the cosmic expansion is faster. However, in order to estimate the conditions to avoid the catastrophe quantitatively, we might have to perform numerical simulations including Higgs-radiation coupling. Moreover, we have mentioned in Sec. 4.3 that the coupling between inflaton and radiation which leads to the complete reheating plays the crucial role. Importantly, the relevant time scale of Higgs dynamics is rather short, and the instantaneous thermalization assumption of radiation might be questionable, in particular for a low reheating temperature. We have roughly estimated its effect in two cases; typical reheating temperature of $T_{\text{RH}} \simeq 10^{10}$ GeV and low reheating temperature of $T_{\text{RH}} \simeq 10^5$ GeV. It was shown that thermal effects might save the electroweak vacuum in the former case after the preheating, while in the latter case, the cosmic expansion kills almost all the parameters required for the

stability of vacuum during inflation. However, since it crucially depends on thermalization processes, further studies are required to obtain quantitative results.

Second, we have assumed that other SM particles than Higgs are produced *perturbatively* via the decay of inflaton, and neglected their resonant production. However, the resonance takes place at the early stage of the complete reheating, for instance, in the case of $(\phi/M_{\text{pl}})\tilde{F}F$ with a sizable coupling, which yields $T_{\text{RH}} \gtrsim \mathcal{O}(10^{10})$ GeV. Their resonant production might affect the stabilization of Higgs during the preheating stage, although its efficiency strongly depends on couplings of inflaton with radiation and inflaton amplitude after the inflation. We leave thorough studies in this respect as a future work.

Third, we comment on the h_{max} dependence of our result. We have used the value $h_{\text{max}} = 10^{10}$ GeV in this paper, but we expect that our result does not change much as long as h_{max} satisfies $\tilde{\lambda}h_{\text{max}}^2 \ll \sqrt{q}m_\phi^2$ or qm_ϕ^2 for the quartic or curvature coupling case, respectively. If the inequality is inverted, the resonance shuts off due to the positive Higgs self-coupling even for a quite large value of the resonance parameter. Thus, Higgs will be trivially stable against the preheating in such a case. Precise determination of the top mass will make the situation clearer in the future.

Fourth, we comment on a possible effect of a tail of the Higgs distribution. In this study, we have estimated the condition where the electroweak vacuum decays on average. In reality, however, we have $e^{3\mathcal{N}}$ numbers of Hubble patches with $\mathcal{N} \simeq 50$ -60, and hence we must estimate the condition at which no one in the $e^{3\mathcal{N}}$ Hubble patches experiences the electroweak vacuum decay. It is possible that the conditions (2.26) and (2.43) are violated in one Hubble patch even if they are satisfied on average since the distribution of the Higgs field value has a tail. Thus, the condition for c and ξ can be even severer once we include this effect. A detailed study on this respect requires a precise knowledge about the distribution of Higgs, and we leave it as a future work.

Fifth, we can generalize our study to the following Planck-suppressed interaction:

$$\mathcal{L}_{\text{int}} = -\frac{h^2}{6M_{\text{pl}}^2} \left[\frac{c_K}{2} \partial_\mu \phi \partial^\mu \phi + c_V V(\phi) \right], \quad (5.1)$$

where $V(\phi)$ is the potential of inflaton, although we have treated only the Higgs-inflaton and -curvature coupling given in Eq. (1.1) in this paper. If $c_K \simeq c_V$, the effective mass term of Higgs induced by this interaction does not oscillate much and hence the resonant Higgs production is expected to be suppressed, leading to weaker constraint.^{♡32} If $c_K \neq c_V$, the effective mass term oscillates with time during the inflaton oscillation regime, and we obtain similar constraints to the case studied in the main text. Note that these couplings generically exist due to, *e.g.* radiative processes. For example, it is discussed in Ref. [79] how the Higgs-inflaton quartic coupling emerges from loop effects in various models. The Higgs-curvature coupling is also generally induced by radiative corrections in the curved space [22].

Finally, we comment on the shape of the inflaton potential. In this paper, we assumed that inflaton oscillates around the origin of the potential, which is typical in high-scale inflation models. However, it is possible that inflaton oscillates around some finite vacuum expectation value (VEV). The result does not change in the case of the Higgs-curvature coupling: we can just regard $\phi(t)$ as the displacement from the VEV. In the case of quartic coupling $c^2\phi^2h^2$, the results depend on the value of inflaton VEV around which the inflaton

^{♡32} Precisely speaking, even if $c_K = c_V$, the energy density of inflaton and the Hubble parameter have oscillating parts at the onset of the oscillation [52].

oscillates. It is expected that the resonant Higgs production effect becomes weaker for larger VEV, although further detailed investigations will be necessary to derive precise constraints on parameters.

Acknowledgments

This work was supported by the Grant-in-Aid for Scientific Research on Scientific Research A (No.26247042 [KN]), Young Scientists B (No. 26800121 [KN]), Innovative Areas (No. 26104009 [KN], No. 15H05888 [KN]), by World Premier International Research Center Initiative (WPI Initiative), MEXT, Japan, by JSPS Research Fellowships for Young Scientists (Y.E. and K.M.), and by the Program for Leading Graduate Schools, MEXT, Japan (Y.E.).

A Mode Expansion

Here we summarize basic properties of the mode expansion of the Higgs field:

$$h(x) = \int \frac{d^3k}{[2\pi a(t)]^{3/2}} [\hat{a}_k h_k(t) e^{ik \cdot x} + \text{H.c.}], \quad (\text{A.1})$$

where \mathbf{k} is the comoving momentum and $a(t)$ is the scale factor. Neglecting interaction terms, we find the equation of motion for the wave function h_k :

$$0 = \ddot{h}_k(t) + [\omega_{k;h}^2(t) + \Delta(t)] h_k(t), \quad (\text{A.2})$$

where $\Delta \equiv -9H^2/4 - 3\dot{H}/2$, $H \equiv \dot{a}/a$ and $\omega_{k;h}(t)$ is the time dependent dispersion relation of Higgs. We take the Wronskian of the Higgs field as

$$h_k \dot{h}_k^* - h_k^* \dot{h}_k = i, \quad (\text{A.3})$$

which fixes the normalization of the wave function. The wave equation leaves the Wronskian invariant since it is linear in h_k . Together with the canonical commutation relation of Higgs, this normalization implies the following algebras for the creation/annihilation operator:

$$[\hat{a}_k, \hat{a}_{k'}^\dagger] = \delta(\mathbf{k} - \mathbf{k}'), \quad [\hat{a}_k, \hat{a}_{k'}] = [\hat{a}_k^\dagger, \hat{a}_{k'}^\dagger] = 0. \quad (\text{A.4})$$

Here note that there is redundancy of the expression in Eq (A.1). We can always rephrase Eq. (A.1) by another set of $(\tilde{a}_k, \tilde{h}_k)$ satisfying $\tilde{a}_k = \alpha_k \hat{a}_k + \beta_k^* \hat{a}_{-k}^\dagger$ and $\tilde{h}_k = \alpha_k^* h_k - \beta_k h_{-k}^*$ under $|\alpha_k|^2 - |\beta_k|^2 = 1$. This is the well-known Bogolyubov transform, $\mathcal{B} : (\hat{a}_k, h_k) \mapsto (\tilde{a}_k, \tilde{h}_k)$, which leaves the Wronskian, commutators and the norm $(h_k, h_{-k}^*) \cdot (\hat{a}_k, \hat{a}_{-k}^\dagger)^t$ invariant. By using this redundancy, one can always take a basis which satisfies the following initial condition:³³

$$h_k(t \rightarrow 0) \rightarrow \frac{1}{\sqrt{2\omega_{k;h}(0)}}, \quad \dot{h}_k(t \rightarrow 0) \rightarrow -i \sqrt{\frac{\omega_{k;h}(0)}{2}}. \quad (\text{A.5})$$

Then, the initial vacuum state is annihilated by the corresponding operator $\hat{a}_k |0; \text{in}\rangle = 0$. We take this basis in the discussion given in this paper. Here we have omitted contributions from the cosmic expansion $\sim \mathcal{O}(H^2/\omega_{k;h}^2)$, that is, we keep the leading order WKB result with respect to the cosmic expansion.

³³ The initial condition should be consistent with the normalization of Wronskian.

B Renormalization in Classical Lattice Simulation

In this appendix, we explain the renormalization procedure we have used in our classical lattice simulations. We follow the procedure given in Refs. [80, 81].

In the classical lattice simulations, we introduce initial gaussian fluctuations originating from the quantum fluctuations for each field. Thus, effective mass terms are induced by these fluctuations. To be concrete, we consider the Lagrangian (3.7) here. Then, the initial mass terms of inflaton, Higgs and χ are given by

$$m_{\text{eff};\phi}^2(0) = m_\phi^2 + \frac{c^2}{2} \int_{\mathbf{k}}^\Lambda G_{F;h}(0, 0; \mathbf{k}) + \delta m_{\Lambda;\phi}^2(0), \quad (\text{B.1})$$

$$m_{\text{eff};h}^2(0) = c^2 \Phi_{\text{ini}}^2 + \frac{1}{2} \int_{\mathbf{k}}^\Lambda \left[c^2 G_{F;\phi}(0, 0; \mathbf{k}) + 3\lambda G_{F;h}(0, 0; \mathbf{k}) + g_{h\chi}^2 G_{F;\chi}(0, 0; \mathbf{k}) \right] + \delta m_{\Lambda;h}^2(0), \quad (\text{B.2})$$

$$m_{\text{eff};\chi}^2(0) = \frac{1}{2} \int_{\mathbf{k}}^\Lambda \left[g_{h\chi}^2 G_{F;h}(0, 0; \mathbf{k}) + 3g_{\chi\chi}^2 G_{F;\chi}(0, 0; \mathbf{k}) \right] + \delta m_{\Lambda;\chi}^2(0), \quad (\text{B.3})$$

where we have included the mass counter terms for inflaton, Higgs and χ . These effective mass terms are UV sensitive since the statistical functions are initially given by

$$\frac{1}{2} G_{F;i}(0, 0; \mathbf{k}) = \frac{1}{2\omega_{k;i}}, \quad (\text{B.4})$$

where $i = \phi, h$ and χ . In the classical lattice simulations, the cut-off scale Λ (or the regularization procedure) is provided by the lattice discretization. Thus, what we have to do here is to renormalize the cut-off scale dependence by the mass counter terms. We choose the mass counter terms such that the contributions from the initial gaussian fluctuations are canceled by them, *i.e.*,

$$\delta m_{\Lambda;\phi}^2(0) = -\frac{c^2}{2} \int_{\mathbf{k}}^\Lambda G_{F;h}(0, 0; \mathbf{k}), \quad (\text{B.5})$$

$$\delta m_{\Lambda;h}^2(0) = -\frac{1}{2} \int_{\mathbf{k}}^\Lambda \left[c^2 G_{F;\phi}(0, 0; \mathbf{k}) + 3\lambda G_{F;h}(0, 0; \mathbf{k}) + g_{h\chi}^2 G_{F;\chi}(0, 0; \mathbf{k}) \right], \quad (\text{B.6})$$

$$\delta m_{\Lambda;\chi}^2(0) = -\frac{1}{2} \int_{\mathbf{k}}^\Lambda \left[g_{h\chi}^2 G_{F;h}(0, 0; \mathbf{k}) + 3g_{\chi\chi}^2 G_{F;\chi}(0, 0; \mathbf{k}) \right], \quad (\text{B.7})$$

for the quartic coupling case. We take the time evolution of the counter terms as

$$\delta m_{\Lambda;i}^2(t) = \frac{m_{\Lambda;i}^2(0)}{a^2(t)}, \quad (\text{B.8})$$

where $i = \phi, h$ and χ . This is because the physical cut-off scale $\Lambda_{\text{cut}}(t)$ evolves as $\Lambda_{\text{cut}}(t) = \Lambda/a(t)$ due to the cosmic expansion. We have also renormalized the mass terms originating from the Higgs self coupling, Higgs- χ coupling and χ self coupling in the same way for the curvature coupling case.

The renormalization procedure described here is unimportant for the analysis in Sec. 2. This is because the Higgs-inflaton couplings c and ξ are small in the case of our interest. However, it is crucial for the study of the annihilation process given in Sec. 3.2, where the couplings $g_{h\chi}$ and $g_{\chi\chi}$ are relatively large, of order $\mathcal{O}(0.1-1)$. See Ref. [81] for more details on the importance of the renormalization procedure in the classical lattice simulations.

C Thermalization after Inflation

In this appendix, we summarize basic properties of thermalization after inflation in the case of the reheating via a Planck-suppressed decay of inflaton. Here we assume that the inflaton decays perturbatively, and neglect the resonant production. The thermalization process in this case is investigated in Refs. [61, 62].^{♡34} We follow the discussion given there.

Suppose that inflaton reheats the Universe via a Planck-suppressed decay, $\Gamma_\phi = \tilde{\Gamma}_\phi m_\phi^3/M_{\text{pl}}^2$ with $\tilde{\Gamma}_\phi \ll 1$. In this case, the number density of radiation right after the decay of inflaton may be given by $n_h \sim \Gamma_\phi n_\phi/H \sim \tilde{\Gamma}_\phi m_\phi^3 (m_\phi t)^{-1}$, which is always smaller than the thermal one; so-called “*under-occupied*” primaries [73]. The bottleneck process is in-medium collinear splittings of hard primaries [73] with the momentum of $p \sim m_\phi$. It is shown that, for $m_\phi t \lesssim \tilde{t}_{\text{max}} \equiv \alpha^{-16/5} \tilde{\Gamma}_\phi^{-3/5}$, these hard primaries cannot participate in thermal plasma, and remain intact. They may yield the following finite density corrections to the Higgs mass:

$$\delta m_{\text{th,h}}^2 \Big|_{\text{hard}} \sim g^2 \tilde{\Gamma}_\phi m_\phi^2 (m_\phi t)^{-1} \quad \text{for } g_{\text{eff}} |h| \ll m_\phi. \quad (\text{C.1})$$

Here $g \sim y_t$ denotes the electroweak gauge coupling and the top Yukawa collectively, to avoid unnecessary complications. Note that $m_\phi t \gg 1$ is required since the inflaton should oscillate once at least so as to decay.

Though the hard primaries dominate the energy and number densities, the soft population is produced via collinear splittings by them. A quantum destructive interference effect prevents emission faster than a time that it takes to resolve the overlaps between the parent and daughter, that is $t \gtrsim k/k_\perp^2 \sim 1/k\theta^2$. In the medium, the daughter acquires transverse momentum by random collisions, $k_\perp^2 \sim \hat{q}_{\text{el}} t$ with $\hat{q}_{\text{el}} \sim \alpha^2 n_h$ being the diffusion constant at that time. Thus, for a given time t , there is an upper bound on the momentum, $k \lesssim k_{\text{form}} \equiv \hat{q}_{\text{el}} t^2$. While a medium induced cascade takes place below k_{form} with a typical angle $\theta \lesssim \alpha^{1/2}$, a vacuum cascade may become relevant above k_{form} with a minimum angle $\theta \gtrsim 1/(kt)^{1/2}$ [83]. On the one hand, if the formation momentum is lower than the Hubble parameter, $k_{\text{form}} \lesssim H$, the finite density corrections to the Higgs mass may be dominated by the vacuum cascade spectrum. On the other hand, for $k_{\text{form}} \gtrsim H$, the LPM-suppressed spectrum and the thermal-like spectrum below $k_{\text{max}} \sim \alpha \tilde{\Gamma}_\phi^{1/2} m_\phi$ provide dominant corrections to the Higgs mass. After a characteristic time scale, $m_\phi t > \tilde{t}_{\text{soft}} \equiv \alpha^{-3} \tilde{\Gamma}_\phi^{-1/2}$, the soft populations are thermalized among themselves. Eventually, for $m_\phi t > \tilde{t}_{\text{max}} \equiv \alpha^{-16/5} \tilde{\Gamma}_\phi^{-3/5}$, the radiation, including hard primaries, is thermalized against the expansion of the Universe, and follows the standard evolution. Thus, the soft population may yield the following corrections to the

^{♡34} See also Ref. [82].

Higgs mass term [61, 62]:^{♡35}

$$\delta m_{\text{th};h}^2 \Big|_{\text{soft}} \sim g^2 \begin{cases} \alpha \tilde{\Gamma}_\phi m_\phi^2 & \text{for } g|h| \ll k_{\text{max}} \sim H; m_\phi t < \tilde{t}_{\text{el}}, \\ \alpha \tilde{\Gamma}_\phi m_\phi^2 \left(\frac{\tilde{t}_{\text{el}}}{m_\phi t} \right)^{\frac{1}{2}} & \text{for } g|h| \ll k_{\text{max}} \sim \alpha \tilde{\Gamma}_\phi^{\frac{1}{2}} m_\phi; \tilde{t}_{\text{el}} < m_\phi t < \tilde{t}_{\text{soft}}, \\ \alpha^2 \tilde{\Gamma}_\phi m_\phi^2 \left(\frac{m_\phi t}{\tilde{t}_{\text{soft}}} \right)^2 & \text{for } g|h| \ll k_{\text{max}} \sim \alpha^4 \tilde{\Gamma}_\phi m_\phi(m_\phi t); \tilde{t}_{\text{soft}} < m_\phi t < \tilde{t}_{\text{max}}, \\ \alpha^{\frac{8}{5}} \tilde{\Gamma}_\phi^{\frac{4}{5}} m_\phi^2 \left(\frac{\tilde{t}_{\text{max}}}{m_\phi t} \right)^{\frac{1}{2}} & \text{for } g|h| \ll k_{\text{max}} \sim \tilde{\Gamma}_\phi^{\frac{1}{4}} m_\phi(m_\phi t)^{-\frac{1}{4}}; \tilde{t}_{\text{max}} < m_\phi t < \tilde{t}_{\text{RH}}. \end{cases} \quad (\text{C.2})$$

Here the time after which medium effects dominate splittings is defined as $\tilde{t}_{\text{el}} = \alpha^{-1} \tilde{\Gamma}_\phi^{-1/2}$; the time after which the soft populations are thermalized is $\tilde{t}_{\text{soft}} = \alpha^{-3} \tilde{\Gamma}_\phi^{-1/2}$; the time after which the radiation is thermalized is $\tilde{t}_{\text{max}} = \alpha^{-16/5} \tilde{\Gamma}_\phi^{-3/5}$; and the time when the reheating is completed is $\tilde{t}_{\text{RH}} = \tilde{\Gamma}_\phi^{-1} M_{\text{pl}}^2 / m_\phi^2$.

References

- [1] M. Sher, “Electroweak Higgs Potentials and Vacuum Stability,” *Phys. Rept.* **179** (1989) 273–418.
- [2] P. B. Arnold, “Can the Electroweak Vacuum Be Unstable?,” *Phys. Rev.* **D40** (1989) 613.
- [3] G. W. Anderson, “New Cosmological Constraints on the Higgs Boson and Top Quark Masses,” *Phys. Lett.* **B243** (1990) 265–270.
- [4] P. B. Arnold and S. Vokos, “Instability of hot electroweak theory: bounds on $m(H)$ and $M(t)$,” *Phys. Rev.* **D44** (1991) 3620–3627.
- [5] J. R. Espinosa and M. Quiros, “Improved metastability bounds on the standard model Higgs mass,” *Phys. Lett.* **B353** (1995) 257–266, [arXiv:hep-ph/9504241 \[hep-ph\]](#).
- [6] G. Isidori, G. Ridolfi, and A. Strumia, “On the metastability of the standard model vacuum,” *Nucl. Phys.* **B609** (2001) 387–409, [arXiv:hep-ph/0104016 \[hep-ph\]](#).
- [7] J. R. Espinosa, G. F. Giudice, and A. Riotto, “Cosmological implications of the Higgs mass measurement,” *JCAP* **0805** (2008) 002, [arXiv:0710.2484 \[hep-ph\]](#).
- [8] J. Ellis, J. R. Espinosa, G. F. Giudice, A. Hoecker, and A. Riotto, “The Probable Fate of the Standard Model,” *Phys. Lett.* **B679** (2009) 369–375, [arXiv:0906.0954 \[hep-ph\]](#).
- [9] F. Bezrukov and M. Shaposhnikov, “Standard Model Higgs boson mass from inflation: Two loop analysis,” *JHEP* **07** (2009) 089, [arXiv:0904.1537 \[hep-ph\]](#).
- [10] J. Elias-Miro, J. R. Espinosa, G. F. Giudice, G. Isidori, A. Riotto, and A. Strumia, “Higgs mass implications on the stability of the electroweak vacuum,” *Phys. Lett.* **B709** (2012) 222–228, [arXiv:1112.3022 \[hep-ph\]](#).

^{♡35} Owing to the Fermi-Dirac statistics, the soft sector is dominated by bosons, *i.e.* SM gauge bosons.

- [11] F. Bezrukov, M. Yu. Kalmykov, B. A. Kniehl, and M. Shaposhnikov, “Higgs Boson Mass and New Physics,” *JHEP* **10** (2012) 140, [arXiv:1205.2893 \[hep-ph\]](#).
- [12] G. Degrassi, S. Di Vita, J. Elias-Miro, J. R. Espinosa, G. F. Giudice, G. Isidori, and A. Strumia, “Higgs mass and vacuum stability in the Standard Model at NNLO,” *JHEP* **08** (2012) 098, [arXiv:1205.6497 \[hep-ph\]](#).
- [13] D. Buttazzo, G. Degrassi, P. P. Giardino, G. F. Giudice, F. Sala, A. Salvio, and A. Strumia, “Investigating the near-criticality of the Higgs boson,” *JHEP* **12** (2013) 089, [arXiv:1307.3536 \[hep-ph\]](#).
- [14] A. V. Bednyakov, B. A. Kniehl, A. F. Pikelner, and O. L. Veretin, “Stability of the Electroweak Vacuum: Gauge Independence and Advanced Precision,” *Phys. Rev. Lett.* **115** no. 20, (2015) 201802, [arXiv:1507.08833 \[hep-ph\]](#).
- [15] V. Branchina and E. Messina, “Stability, Higgs Boson Mass and New Physics,” *Phys. Rev. Lett.* **111** (2013) 241801, [arXiv:1307.5193 \[hep-ph\]](#).
- [16] V. Branchina, E. Messina, and A. Platania, “Top mass determination, Higgs inflation, and vacuum stability,” *JHEP* **09** (2014) 182, [arXiv:1407.4112 \[hep-ph\]](#).
- [17] V. Branchina, E. Messina, and M. Sher, “Lifetime of the electroweak vacuum and sensitivity to Planck scale physics,” *Phys. Rev.* **D91** (2015) 013003, [arXiv:1408.5302 \[hep-ph\]](#).
- [18] A. Kobakhidze and A. Spencer-Smith, “Electroweak Vacuum (In)Stability in an Inflationary Universe,” *Phys. Lett.* **B722** (2013) 130–134, [arXiv:1301.2846 \[hep-ph\]](#).
- [19] M. Fairbairn and R. Hogan, “Electroweak Vacuum Stability in light of BICEP2,” *Phys. Rev. Lett.* **112** (2014) 201801, [arXiv:1403.6786 \[hep-ph\]](#).
- [20] A. Hook, J. Kearney, B. Shakya, and K. M. Zurek, “Probable or Improbable Universe? Correlating Electroweak Vacuum Instability with the Scale of Inflation,” *JHEP* **01** (2015) 061, [arXiv:1404.5953 \[hep-ph\]](#).
- [21] K. Kamada, “Inflationary cosmology and the standard model Higgs with a small Hubble induced mass,” *Phys. Lett.* **B742** (2015) 126–135, [arXiv:1409.5078 \[hep-ph\]](#).
- [22] M. Herranen, T. Markkanen, S. Nurmi, and A. Rajantie, “Spacetime curvature and the Higgs stability during inflation,” *Phys. Rev. Lett.* **113** no. 21, (2014) 211102, [arXiv:1407.3141 \[hep-ph\]](#).
- [23] J. Kearney, H. Yoo, and K. M. Zurek, “Is a Higgs Vacuum Instability Fatal for High-Scale Inflation?,” *Phys. Rev.* **D91** no. 12, (2015) 123537, [arXiv:1503.05193 \[hep-th\]](#).
- [24] J. R. Espinosa, G. F. Giudice, E. Morgante, A. Riotto, L. Senatore, A. Strumia, and N. Tetradis, “The cosmological Higgstory of the vacuum instability,” *JHEP* **09** (2015) 174, [arXiv:1505.04825 \[hep-ph\]](#).
- [25] L. Kofman, A. D. Linde, and A. A. Starobinsky, “Reheating after inflation,” *Phys. Rev. Lett.* **73** (1994) 3195–3198, [arXiv:hep-th/9405187 \[hep-th\]](#).
- [26] L. Kofman, A. D. Linde, and A. A. Starobinsky, “Towards the theory of reheating after inflation,” *Phys. Rev.* **D56** (1997) 3258–3295, [arXiv:hep-ph/9704452 \[hep-ph\]](#).
- [27] A. D. Dolgov and D. P. Kirilova, “ON PARTICLE CREATION BY A TIME DEPENDENT SCALAR FIELD,” *Sov. J. Nucl. Phys.* **51** (1990) 172–177. [*Yad. Fiz.*51,273(1990)].

- [28] J. H. Traschen and R. H. Brandenberger, “Particle Production During Out-of-equilibrium Phase Transitions,” *Phys. Rev.* **D42** (1990) 2491–2504.
- [29] Y. Shtanov, J. H. Traschen, and R. H. Brandenberger, “Universe reheating after inflation,” *Phys. Rev.* **D51** (1995) 5438–5455, [arXiv:hep-ph/9407247](#) [hep-ph].
- [30] B. A. Bassett and S. Liberati, “Geometric reheating after inflation,” *Phys. Rev.* **D58** (1998) 021302, [arXiv:hep-ph/9709417](#) [hep-ph]. [Erratum: *Phys. Rev.* D60,049902(1999)].
- [31] S. Tsujikawa, K.-i. Maeda, and T. Torii, “Resonant particle production with nonminimally coupled scalar fields in preheating after inflation,” *Phys. Rev.* **D60** (1999) 063515, [arXiv:hep-ph/9901306](#) [hep-ph].
- [32] M. Herranen, T. Markkanen, S. Nurmi, and A. Rajantie, “Spacetime curvature and Higgs stability after inflation,” *Phys. Rev. Lett.* **115** (2015) 241301, [arXiv:1506.04065](#) [hep-ph].
- [33] I. Affleck, “Quantum Statistical Metastability,” *Phys. Rev. Lett.* **46** (1981) 388.
- [34] A. D. Linde, “Decay of the False Vacuum at Finite Temperature,” *Nucl. Phys.* **B216** (1983) 421. [Erratum: *Nucl. Phys.* B223,544(1983)].
- [35] **ATLAS, CDF, CMS, DO** Collaboration, “First combination of Tevatron and LHC measurements of the top-quark mass,” [arXiv:1403.4427](#) [hep-ex].
- [36] **Planck** Collaboration, P. A. R. Ade *et al.*, “Planck 2015 results. XX. Constraints on inflation,” [arXiv:1502.02114](#) [astro-ph.CO].
- [37] F. L. Bezrukov and M. Shaposhnikov, “The Standard Model Higgs boson as the inflaton,” *Phys. Lett.* **B659** (2008) 703–706, [arXiv:0710.3755](#) [hep-th].
- [38] K. Nakayama and F. Takahashi, “Running Kinetic Inflation,” *JCAP* **1011** (2010) 009, [arXiv:1008.2956](#) [hep-ph].
- [39] C. Destri, H. J. de Vega, and N. G. Sanchez, “MCMC analysis of WMAP3 and SDSS data points to broken symmetry inflaton potentials and provides a lower bound on the tensor to scalar ratio,” *Phys. Rev.* **D77** (2008) 043509, [arXiv:astro-ph/0703417](#) [astro-ph].
- [40] K. Nakayama, F. Takahashi, and T. T. Yanagida, “Polynomial Chaotic Inflation in the Planck Era,” *Phys. Lett.* **B725** (2013) 111–114, [arXiv:1303.7315](#) [hep-ph].
- [41] R. Kallosh and A. Linde, “Universality Class in Conformal Inflation,” *JCAP* **1307** (2013) 002, [arXiv:1306.5220](#) [hep-th].
- [42] R. Kallosh, A. Linde, and D. Roest, “Superconformal Inflationary α -Attractors,” *JHEP* **11** (2013) 198, [arXiv:1311.0472](#) [hep-th].
- [43] G. Baym and L. P. Kadanoff, *Quantum statistical mechanics*, vol. 1. WA Benjamin, New York, 1962.
- [44] K.-c. Chou, Z.-b. Su, B.-l. Hao, and L. Yu, “Equilibrium and Nonequilibrium Formalisms Made Unified,” *Phys.Rept.* **118** (1985) 1.
- [45] E. Calzetta and B. Hu, “Nonequilibrium Quantum Fields: Closed Time Path Effective Action, Wigner Function and Boltzmann Equation,” *Phys.Rev.* **D37** (1988) 2878.
- [46] J. Berges, “Introduction to nonequilibrium quantum field theory,” *AIP Conf.Proc.* **739** (2005) 3–62, [arXiv:hep-ph/0409233](#) [hep-ph].

- [47] E. A. Calzetta and B.-L. Hu, *Nonequilibrium quantum field theory*, vol. 10. Cambridge University Press, 2008.
- [48] G. Aarts and J. Berges, “Classical aspects of quantum fields far from equilibrium,” *Phys. Rev. Lett.* **88** (2002) 041603, [arXiv:hep-ph/0107129](#) [hep-ph].
- [49] P. R. Anderson, C. Molina-Paris, and E. Mottola, “Short distance and initial state effects in inflation: Stress tensor and decoherence,” *Phys. Rev.* **D72** (2005) 043515, [arXiv:hep-th/0504134](#) [hep-th].
- [50] A. Tranberg, “Quantum field thermalization in expanding backgrounds,” *JHEP* **11** (2008) 037, [arXiv:0806.3158](#) [hep-ph].
- [51] L. H. Ford, “Gravitational Particle Creation and Inflation,” *Phys. Rev.* **D35** (1987) 2955.
- [52] Y. Ema, R. Jinno, K. Mukaida, and K. Nakayama, “Gravitational Effects on Inflaton Decay,” *JCAP* **1505** no. 05, (2015) 038, [arXiv:1502.02475](#) [hep-ph].
- [53] G. N. Felder and I. Tkachev, “LATTICEEASY: A Program for lattice simulations of scalar fields in an expanding universe,” *Comput. Phys. Commun.* **178** (2008) 929–932, [arXiv:hep-ph/0011159](#) [hep-ph].
- [54] D. Polarski and A. A. Starobinsky, “Semiclassicality and decoherence of cosmological perturbations,” *Class. Quant. Grav.* **13** (1996) 377–392, [arXiv:gr-qc/9504030](#) [gr-qc].
- [55] S. Yu. Khlebnikov and I. I. Tkachev, “Classical decay of inflaton,” *Phys. Rev. Lett.* **77** (1996) 219–222, [arXiv:hep-ph/9603378](#) [hep-ph].
- [56] J. F. Dufaux, G. N. Felder, L. Kofman, M. Peloso, and D. Podolsky, “Preheating with trilinear interactions: Tachyonic resonance,” *JCAP* **0607** (2006) 006, [arXiv:hep-ph/0602144](#) [hep-ph].
- [57] G. N. Felder, L. Kofman, and A. D. Linde, “Instant preheating,” *Phys. Rev.* **D59** (1999) 123523, [arXiv:hep-ph/9812289](#) [hep-ph].
- [58] F. Bezrukov, D. Gorbunov, and M. Shaposhnikov, “On initial conditions for the Hot Big Bang,” *JCAP* **0906** (2009) 029, [arXiv:0812.3622](#) [hep-ph].
- [59] T. Moroi, K. Mukaida, K. Nakayama, and M. Takimoto, “Scalar Trapping and Saxion Cosmology,” *JHEP* **06** (2013) 040, [arXiv:1304.6597](#) [hep-ph].
- [60] G. F. Giudice, E. W. Kolb, and A. Riotto, “Largest temperature of the radiation era and its cosmological implications,” *Phys. Rev.* **D64** (2001) 023508, [arXiv:hep-ph/0005123](#) [hep-ph].
- [61] K. Harigaya and K. Mukaida, “Thermalization after/during Reheating,” *JHEP* **05** (2014) 006, [arXiv:1312.3097](#) [hep-ph].
- [62] K. Mukaida and M. Yamada, “Thermalization Process after Inflation and Effective Potential of Scalar Field,” *JCAP* **1602** no. 02, (2016) 003, [arXiv:1506.07661](#) [hep-ph].
- [63] K. Mukaida and K. Nakayama, “Dynamics of oscillating scalar field in thermal environment,” *JCAP* **1301** (2013) 017, [arXiv:1208.3399](#) [hep-ph].
- [64] K. Mukaida and K. Nakayama, “Dissipative Effects on Reheating after Inflation,” *JCAP* **1303** (2013) 002, [arXiv:1212.4985](#) [hep-ph].

- [65] S. R. Coleman and E. J. Weinberg, “Radiative Corrections as the Origin of Spontaneous Symmetry Breaking,” *Phys. Rev.* **D7** (1973) 1888–1910.
- [66] O. Lebedev and A. Westphal, “Metastable Electroweak Vacuum: Implications for Inflation,” *Phys. Lett.* **B719** (2013) 415–418, [arXiv:1210.6987 \[hep-ph\]](#).
- [67] O. Lebedev, “On Stability of the Electroweak Vacuum and the Higgs Portal,” *Eur. Phys. J.* **C72** (2012) 2058, [arXiv:1203.0156 \[hep-ph\]](#).
- [68] J. Elias-Miro, J. R. Espinosa, G. F. Giudice, H. M. Lee, and A. Strumia, “Stabilization of the Electroweak Vacuum by a Scalar Threshold Effect,” *JHEP* **06** (2012) 031, [arXiv:1203.0237 \[hep-ph\]](#).
- [69] K. Mukaida and K. Nakayama, “Dark Matter Chaotic Inflation in Light of BICEP2,” *JCAP* **1408** (2014) 062, [arXiv:1404.1880 \[hep-ph\]](#).
- [70] G. N. Felder and L. Kofman, “The Development of equilibrium after preheating,” *Phys. Rev.* **D63** (2001) 103503, [arXiv:hep-ph/0011160 \[hep-ph\]](#).
- [71] D. G. Figueroa, J. Garcia-Bellido, and F. Torrenti, “Decay of the standard model Higgs field after inflation,” *Phys. Rev.* **D92** no. 8, (2015) 083511, [arXiv:1504.04600 \[astro-ph.CO\]](#).
- [72] K. Enqvist, S. Nurmi, S. Rusak, and D. Weir, “Lattice Calculation of the Decay of Primordial Higgs Condensate,” *JCAP* **1602** no. 02, (2016) 057, [arXiv:1506.06895 \[astro-ph.CO\]](#).
- [73] A. Kurkela and G. D. Moore, “Thermalization in Weakly Coupled Nonabelian Plasmas,” *JHEP* **12** (2011) 044, [arXiv:1107.5050 \[hep-ph\]](#).
- [74] L. Delle Rose, C. Marzo, and A. Urbano, “On the fate of the Standard Model at finite temperature,” [arXiv:1507.06912 \[hep-ph\]](#).
- [75] R. Micha and I. I. Tkachev, “Relativistic turbulence: A Long way from preheating to equilibrium,” *Phys. Rev. Lett.* **90** (2003) 121301, [arXiv:hep-ph/0210202 \[hep-ph\]](#).
- [76] R. Micha and I. I. Tkachev, “Turbulent thermalization,” *Phys. Rev.* **D70** (2004) 043538, [arXiv:hep-ph/0403101 \[hep-ph\]](#).
- [77] J. Berges, A. Rothkopf, and J. Schmidt, “Non-thermal fixed points: Effective weak-coupling for strongly correlated systems far from equilibrium,” *Phys. Rev. Lett.* **101** (2008) 041603, [arXiv:0803.0131 \[hep-ph\]](#).
- [78] J. Berges and D. Sexty, “Bose condensation far from equilibrium,” *Phys. Rev. Lett.* **108** (2012) 161601, [arXiv:1201.0687 \[hep-ph\]](#).
- [79] C. Gross, O. Lebedev, and M. Zatta, “Higgs-inflaton coupling from reheating and the metastable Universe,” *Phys. Lett.* **B753** (2016) 178–181, [arXiv:1506.05106 \[hep-ph\]](#).
- [80] A. Rajantie, P. M. Saffin, and E. J. Copeland, “Electroweak preheating on a lattice,” *Phys. Rev.* **D63** (2001) 123512, [arXiv:hep-ph/0012097 \[hep-ph\]](#).
- [81] J. Berges, K. Boguslavski, S. Schlichting, and R. Venugopalan, “Basin of attraction for turbulent thermalization and the range of validity of classical-statistical simulations,” *JHEP* **05** (2014) 054, [arXiv:1312.5216 \[hep-ph\]](#).
- [82] J. Ellis, M. A. G. Garcia, D. V. Nanopoulos, K. A. Olive, and M. Peloso, “Post-Inflationary Gravitino Production Revisited,” [arXiv:1512.05701 \[astro-ph.CO\]](#).
- [83] A. Kurkela and U. A. Wiedemann, “Picturing perturbative parton cascades in QCD matter,” *Phys. Lett.* **B740** (2015) 172–178, [arXiv:1407.0293 \[hep-ph\]](#).